AD-A105 529 SOUTHWEST RESEARCH INST SAN ANTONIO TX F/G 11/6
CRACK TIP PLASTICITY ASSOCIATED WITH CORROSION ASSISTED FATIGUE--ETC(U)
SEP 81 D L DAVIDSON, J LANKFORD N00014-75-C-1038
UNCLASSIFIED NL

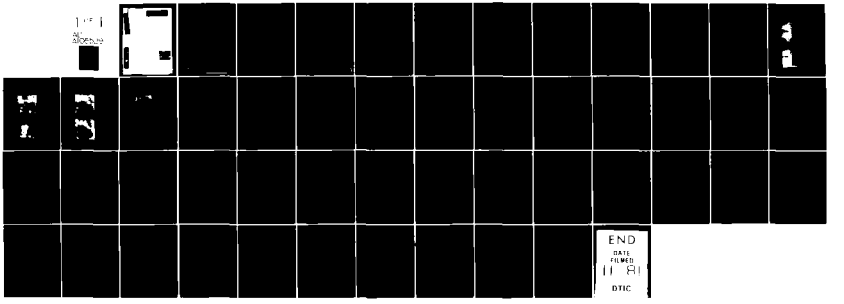

SOUTHWEST RESEARCH INSTITUTE

POST OFFICE DRAWER 28510 · 6220 CULEBRA ROAD · SAN ANTONIO, TEXAS 78284 · (512) 684-5111

(6)

CRACK TIP PLASTICITY ASSOCIATED WITH CORROSION ASSISTED FATIGUE.

(9) INTERIM REPORT FOR PERIOD JUNE 1980 — JUNE 1981

(15) [illegible]-75-C-[illegible]

by

(1) D. L./Davidson
J./Lankford

Prepared for

Office of Naval Research
800 North Quincy Street
Arlington, Virginia 22217

RE: 02-4268
This is a project number and not a report number

(11) 18 Sept[illegible] 1981 (12) 54

328200 (D

SUMMARY

Preliminary data is presented on the effect of a water vapor environment on the deformation within the plastic zone of fatigue cracks in 7075-T6. Results in the water vapor environment is compared to those in a vacuum environment. High spatial resolution observations have been made using a special cyclic stage for the SEM and strains have been determined using the stereoimaging technique. Crack tip opening is shown to be a power function of the distance behind the crack tip, in agreement with a theoretical derivation of this correlation. The crack tip strain correlates with the crack opening at 1 micrometer behind the crack tip. Crack tip strains are shown to vary considerably for a fixed cyclic stress intensity. By ignoring some data, a preliminary analysis is made which indicates that the water vapor environment lowers crack tip strains. Strain distribution within the plastic zone is shown to fit a logarithmic function, as opposed to a power function, although there is still some uncertainty in this result. Work on 7075-T6 and the powder metallurgy alloy MA-87 is continuing, with definitive results expected next year.

TABLE OF CONTENTS

I. INTRODUCTION

Fatigue crack growth in various materials and environments can be correlated empirically (for intermediate crack growth rates) on the basis of the well known Paris law

$$da/dN = A\Delta K^n \quad (1)$$

where da/dN is crack extension per cycle, ΔK is the cyclic stress intensity, and A and n are constants. In the absence of an environmental effect, i.e., in a vacuum or inert gas, n for aluminum alloys usually turns out to be approximately 4.[1] Irving and McCartney, in reviewing[1] the many theoretical models which have been proposed to explain the success of equation (1) have noted that only three kinds of laws predict n=4, in particular, ones based on either (1) damage accumulation, (2) strain accumulation, or (3) energy dissipation. That being the case, one is led to suspect that when aggressive environments modify cyclic crack growth in aluminum alloys, the environmental constituents do so by interacting in some way with the plastic processes taking place at the crack tip. In this section, current evidence of such interaction is reviewed.

Many studies have shown that environments such as humid air accelerate fatigue crack growth rates over those observed in vacuum.[12] Although some of this work has been interpreted in terms of inferred environment-altered deformation processes, we shall not be concerned here with such indirect evidence. Rather, attention will be focussed upon the relatively few investigations which have attempted to characterize directly the crack tip plasticity of aluminum alloys in air versus vacuum environments.

Some idea of the relative extents of plasticity in these two situations has been inferred rather crudely, by simply observing the distribution of slip bands adjacent to the edges of fatigue cracks. For example, Bouchet and de Fouguet[3] observed optically that for Al-4Cu, the spatial extent of the zone of slip trace formation adjacent to cracks growing at identical stress intensities is larger in vacuum than in air. It has further been determined, for both Al-4Cu[4] and Al-3Mg,[5] that the density of such slip bands is higher in vacuum. These observations in combination suggest that in comparison with air tests, plastic strains are more extensive and intense at crack tips growing in a vacuum environment. On the other hand, it should be noted that these measurements really relate to regions closely adjacent to the crack tip, i.e., they do not prove that the macroscopic plastic zone size has been altered. Microhardness tests, however, do provide support for the idea of long range plastic zone changes. In particular, it has been shown,[3] for Al-4Cu, that the plastic zone formed under vacuum has a higher hardness than the equivalent (same stress intensity) zone formed in air, and that the former high hardness zone extends further away from the crack than does the latter. These results imply higher strains, and also greater strain hardening, at the tips of cracks grown in vacuum. Careful study of the original data for these measurements suggests, however, that the results are most conclusive insofar as concerns the alteration of the magnitude of plasticity very near the crack tip; whether the macroscopic plastic zone size really changes is much more difficult to discern.

Despite this good evidence of the presence of environment-induced differences in crack tip plasticity, it is relevant to ask whether such differences per se really alter crack growth, or are they mere by-products of environmental interactions local to the crack tip which, in changing the rate of growth, incidentally change the plastic zone characteristics. Support for the active role of crack tip plasticity in controlling the rate of crack extension can be derived from the results of experiments by Grinberg, et al.[6] The significance of these experiments is based on two known facts. First, over a certain cyclic stress intensity range, aluminum alloys tested in air exhibit crack growth striations on their fracture surfaces; when cycled in vacuum over the same stress intensity range, striations are irregular and faint, if present at all. Second, a reduction in temperature during in vacuum cyclic crack growth of aluminum alloys has been shown to result in a decrease in plastic zone size. In their experiments, Grinberg et al[6] observed crack growth in Al-6Mg. At 23°C, striations were sharp and regular in the fatigue zone of air-tested specimens, but were rare and indistinct in vacuum-tested samples. Reduction of the temperature of the vacuum cyclic tests to -120°C produced sharp, regular striations identical in spacing and appearance to those formed in air at 23°C. Considering that aluminum alloys such as this exhibit only limited strain hardening, the principal effect of the temperature change probably was a reduction in ductility. By direct analogy, the principal effect of air at 23°C is inferred to be a reduction of the ductility of the material within the crack tip plastic zone.

Other studies both agree and disagree with this picture. Although Grinberg, et al, observed identical striation spacings for air tests at 23°C and vacuum experiments at -120°C, they did not report on growth rates, i.e., whether the vacuum growth rate was increased by lowering the temperature. Vogelsang and Schijve,[7] on the other hand, found that lowering the temperature during vacuum fatigue crack growth tests of 7075-T6 and 2024-T3 aluminum alloys had no appreciable effect upon $^{da}/_{dN}$. Further, Louwaard[8] observed that for fine-grained 7075-T6, the vacuum crack growth rate increased with decreasing temperature (basically agreeing with inferences derived from the Grinberg, et al,[6] study), but decreased with decreasing temperature for coarse-grained material.

It is possible to consider crack tip plasticity and environmental interaction from another viewpoint. Crack closure is thought to be a consequence of residual plastic deformation which originally occur in the crack tip region. Both Ewalds[9] and Schijve and Arkema[10] have found crack tip opening stress level, as measured by COD gages, to be independent of environment. On this basis, it was concluded that the macroscopic plastic zone size was not altered by the environment. It was noted, however, that the relative degree of tensile to shear mode deformation, as determined fractographically, is severely altered by the environment. This was taken[9] to imply that while long range plasticity, as inferred from COD measurements, may be environmentally independent, the local crack tip plastic strain amplitude and/or plastic work is environment sensitive.

In summary, several observations have been made regarding possible environmental interaction with crack tip plasticity; two of these issues will be explored in the experimental program outlined in the next section, i.e.,

(1) Whether plastic strains very local to the crack tip are decreased by an air environment.

(2) Whether strain hardening about the crack tip is decreased by an air environment.

Other questions raised in this review will be dealt with in a subsequent report.

II. EXPERIMENTAL PROCEDURE

Fatigue cracks were grown in single edge notched specimens of 7075-T6 and MA-87* aluminum alloys in two environments: 100% relative humidity, termed "wet", and vacuum of approximately 10^{-5} torr, termed "dry". Crack growth rate vs ΔK was measured with ever increasing ΔK (constant load) for both environments in both materials with $R \cong 0.1$, and at a frequency of 10 Hz. Resulting crack growth curves are shown in Figures 1 and 2.

For the 7075-T6 crack tip plasticity experiments, three stress intensity factors were examined: $\Delta K = 6$, 8, and 10 $MN/m^{3/2}$ with $R \cong 0.1$, and frequencies of 1 to 5 Hz; analysis of MA-87 is still in progress. Environments were alternated as necessary to obtain the desired data, and it was determined that crack growth rates changed as expected, according to the curves in Figures 1 and 2. For the "wet" environment, a small chamber surrounding the specimen and grips was used to contain air saturated with water vapor which was flowed through the chamber. The "dry" environment was a diffusion pumped system containing specimen and grips.

After cracks were grown under the conditions desired, the specimen was transferred to a scanning electron microscope cyclic loading stage.[11] When crack growth had taken place in the "wet" environment, photographs of the crack tip region were made on the first cycle at both the minimum and maximum stress intensities. Subsequent cycling in the SEM did not reveal any sudden change in the crack tip characteristics, but for cracks grown in the wet environment, only data taken on the first cycle was used for analysis. For the dry (vacuum) environment, the crack was often studied both on the first cycle and subsequent cycles in the SEM; again, no sudden change was found due to cycling in the SEM.

---

*MA-87 is an experimental alloy produced by powder metallurgy techniques by Alcoa. It is now designated X-7091. Samples were obtained courtesy of Alcoa. The chemical composition of MA-87 closely resembles that of 7075, but the dispersoid content is different and the grain size is much smaller than that of commercial 7075.

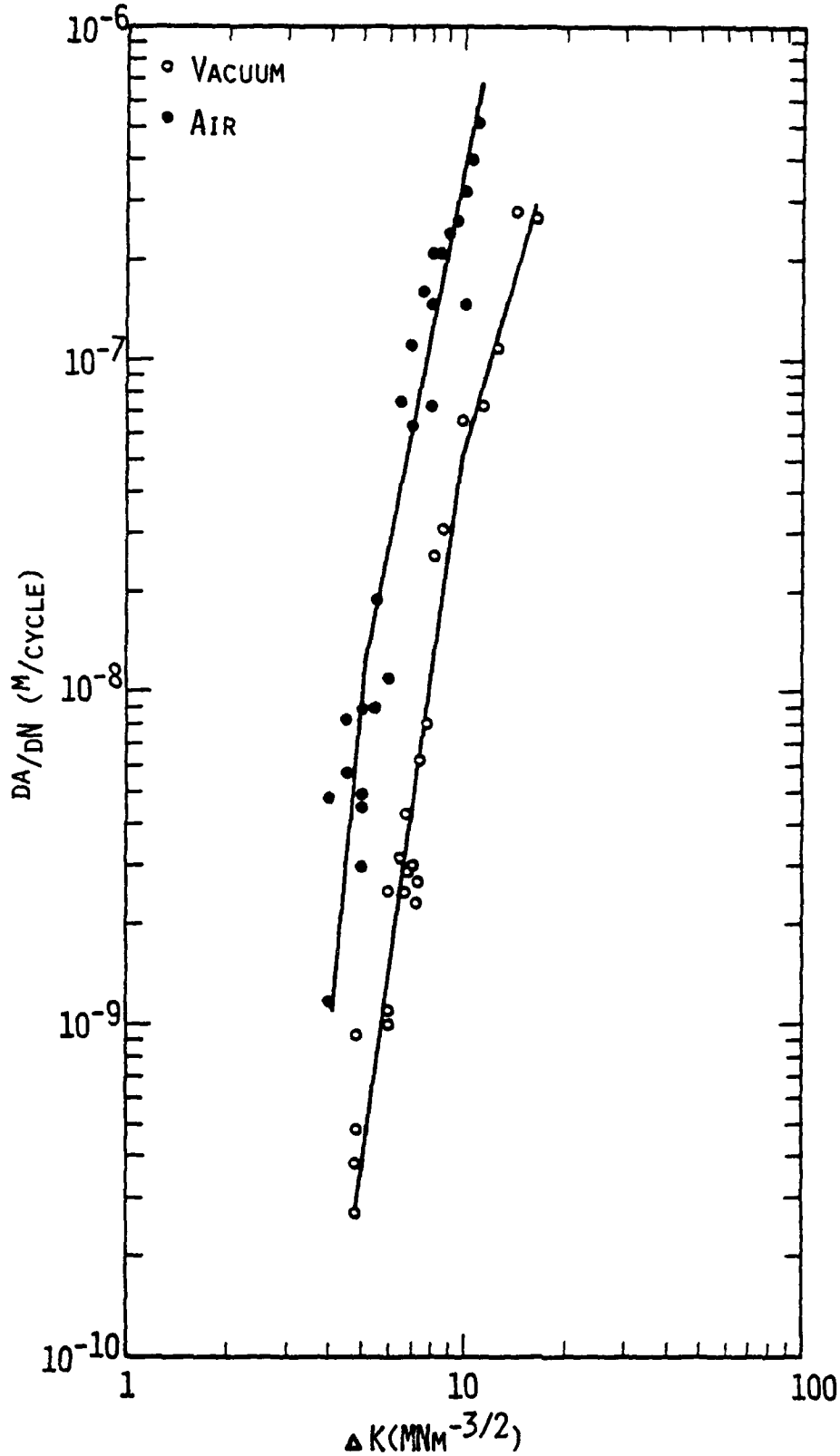

Figure 1. Crack growth rate vs cyclic stress intensity factor: 7075-T6. Wet air environment (50% RH) and vacuum (10^{-5} torr).

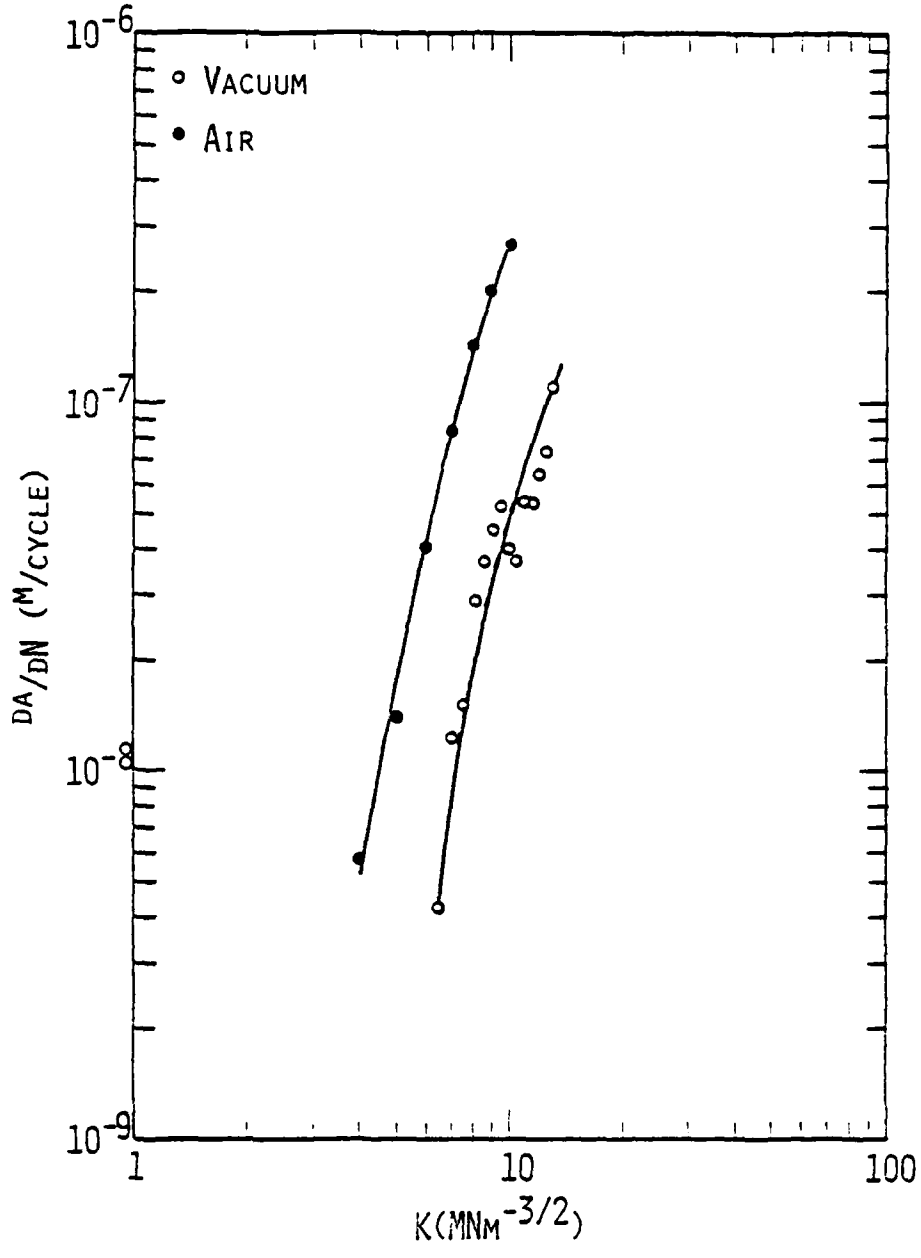

Figure 1. Crack growth rate vs cyclic stress intensity factor: MA-87. Humid air environment (50% RH) and vacuum (10^{-5} torr).

Examples of photographs for both environments are shown in Figures 3-6 at $\Delta K = 6$ and 10 $MN/m^{3/2}$.

The photographs made at the load cycling limits were then compared, using the stereoimaging technique,[12] and the displacements measured at numerous points in the near crack tip field. Examples of the displacements, derived from Figures 3-6, are given in Appendix A. From these measured displacements, three elements of the symmetric strain tensor were computed: $\Delta\varepsilon_{xx}$, $\Delta\varepsilon_{yy}$ and $\Delta\gamma_{xy}$,[13] the normal strains. By using a Mohr's circle construction, the maximum and minimum principal strain ranges, $\Delta\varepsilon_1$ and $\Delta\varepsilon_2$, and the maximum shear strain range, $\Delta\gamma_{max}$, may be computed at each point of measurement. These maximum strain values and normal strain values are shown in Mohr's circles, as derived from Figures 3-6 in Appendix B. Also, the effective strain range

$$\Delta\varepsilon_t^{eff} = \frac{2}{\sqrt{3}} [\Delta\varepsilon_1^{\,2} + \Delta\varepsilon_1\Delta\varepsilon_2 + \Delta\varepsilon_2^{\,2}]^{1/2} \qquad (2)$$

may be computed. This value is the effective value of the total strains and is used to combine several values of strain into one parameter.

III. RESULTS

The results presented here are all those obtained to date on 7075-T6. The data are voluminous, with the opportunity for considerable analysis; however, the analysis of all data and the interpretation of all results are not yet complete. The results presented should, therefore, be considered as preliminary.

Measurements of crack opening magnitude vs distance behind the crack tip are shown in Figures 7-9 for the three stress intensities studied. These data, combined with similar information from 304SS obtained down to 1 μm behind the crack tip, indicate that crack opening C is a power function of the distance behind the crack tip, -y, so that

$$C = C_o|-y|^p \qquad (3)$$

Values of the constants C_o and p derived from Figures 7-9 are given in Table I, along with values of the crack tip effective strain range $\Delta\varepsilon_t^{eff}$. No correlation is evident between the exponent p and ΔK or environment, but C_o appears to be related to $\Delta\varepsilon_t^{eff}$, as shown in Figure 10. The line fit through the data is by linear regression excluding the datum of Set 43.

TABLE I

7075-T6
CRACK OPENING, CRACK TIP STRAIN AND STRAIN DISTRIBUTION PARAMETERS

Set	ΔK $MN/m^{3/2}$	Environment	Crack Tip C_o μm	p	$\Delta\varepsilon_t^{eff}(o)$	Strain Distribution m	$\Delta\varepsilon_o$	A μm
34	6	Dry	.15	.67	.0401	.0068	.0416	1.26
35	6	Dry	.25	.64	.0693	.0093	.0514	.146
36	6.2	Dry	.11	.60	.0484	.0075	.0463	.756
37	6	Wet	.24	.60	.0813	.0168	.0654	.390
38	6	Wet	.077	.60	.0216	.0046	.0249	2.05
39	8	Dry	.097	.72	.0405	.00525	.0306	.152
40	8	Dry	.064	.77	.0415	.00556	.0351	.085
41	8	Dry	.25	.81	.1148	.0310	.1269	1.26
42	8	Wet	.20	.81	.0712	.0123	.0581	.30
43	10	Dry	1.59	.34	.2954	.0738	.2802	.810
44	10	Dry	.52	.60	.1630	.0342	.1444	.580
45	10	Wet	.44	.62	.1609	.0379	.1482	.715

$C = C_o|-y|^p$

$\Delta\varepsilon_t^{eff} = \Delta\varepsilon_o - m \ln(r + A)$

For $\theta = 0°$, ahead of crack

r (μm)

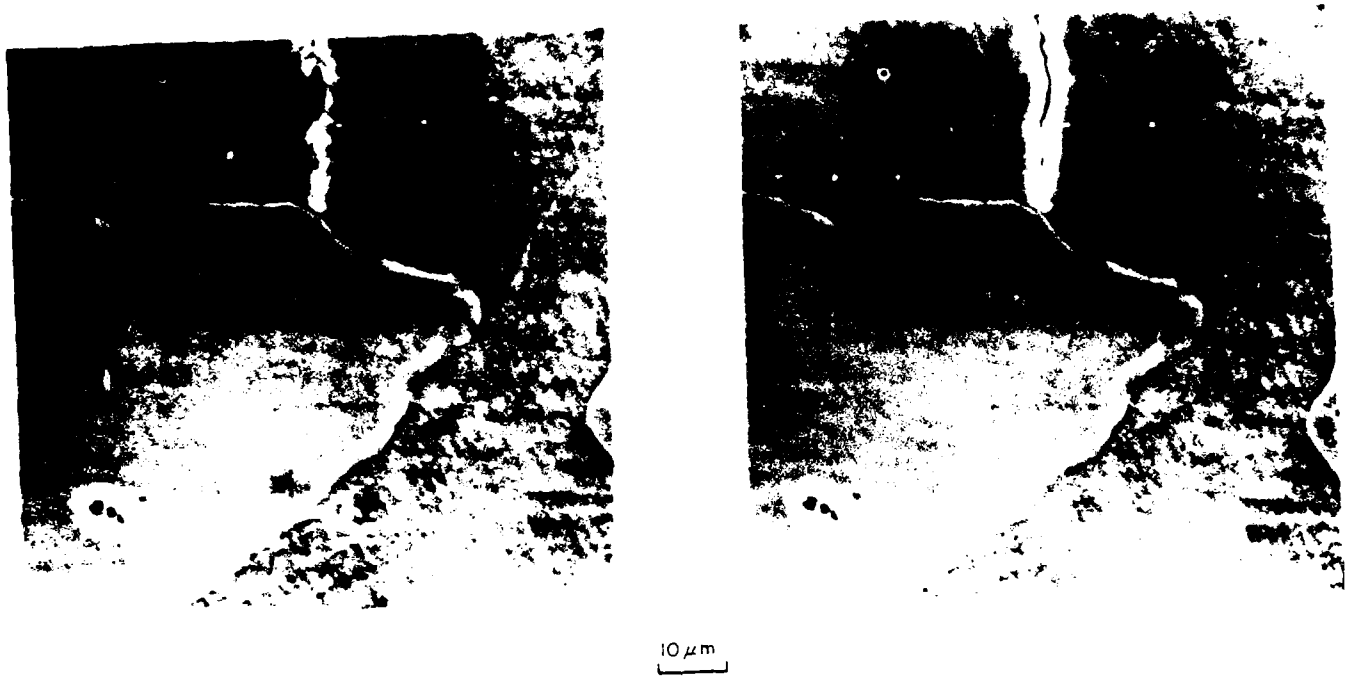

Figure 3. 7075-T6, $\Delta K = 6\ MN/m^{3/2}$, R = 0.15, vacuum environment. Set 35.
Left: minimum load. Right: maximum load.

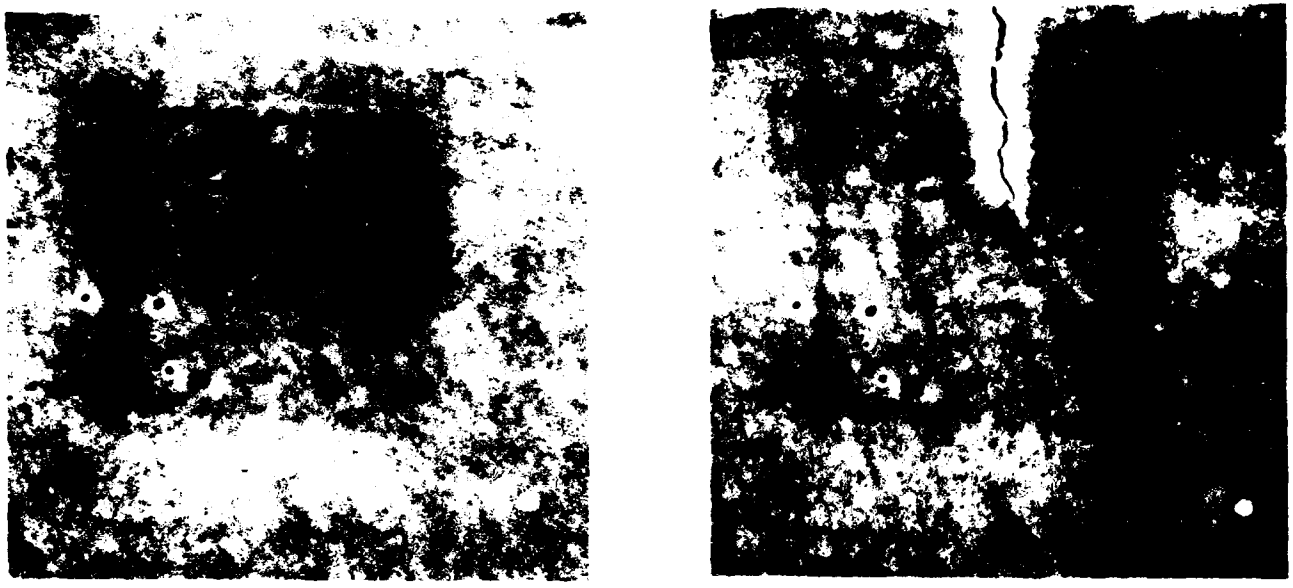

Figure 4. 7075-T6, $\Delta K = 6\ MN/m^{3/2}$, R = 0.15, wet air environment. Set 37.
Left: minimum load. Right: maximum load.

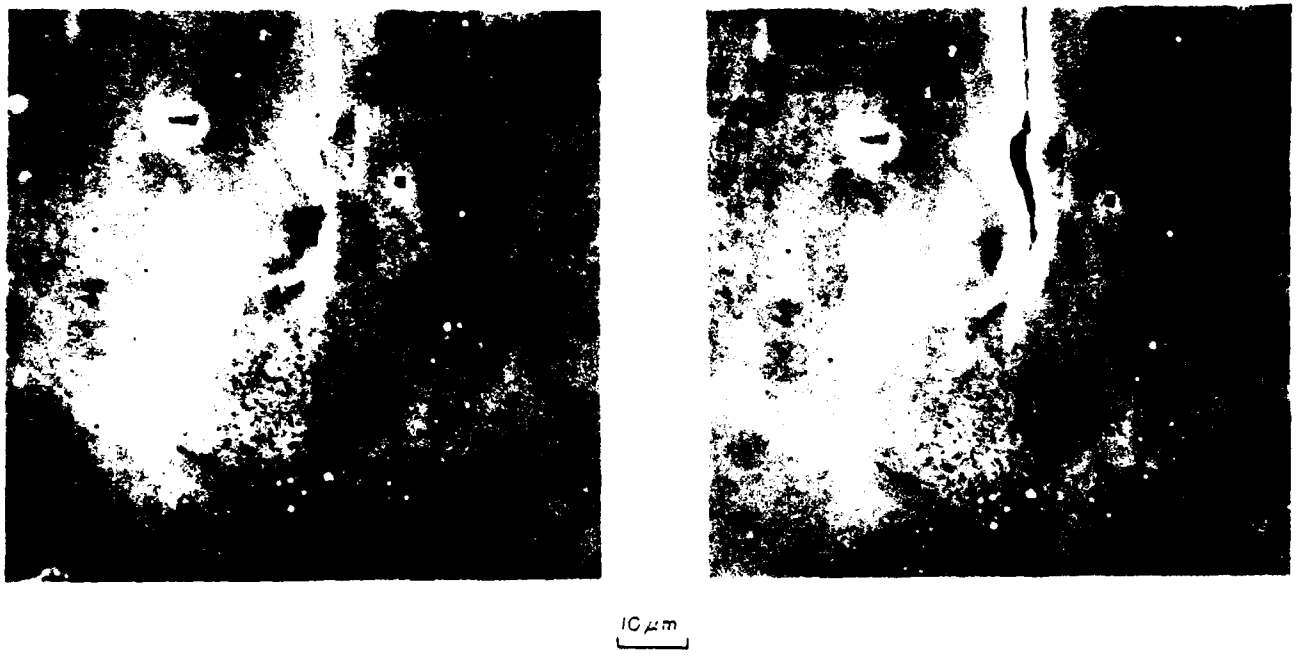

Figure 5. 7075-T6, $\Delta K = 10\ MN/m^{3/2}$, R = 0.25, vacuum environment. Set 43.
Left: minimum load. Right: maximum load.

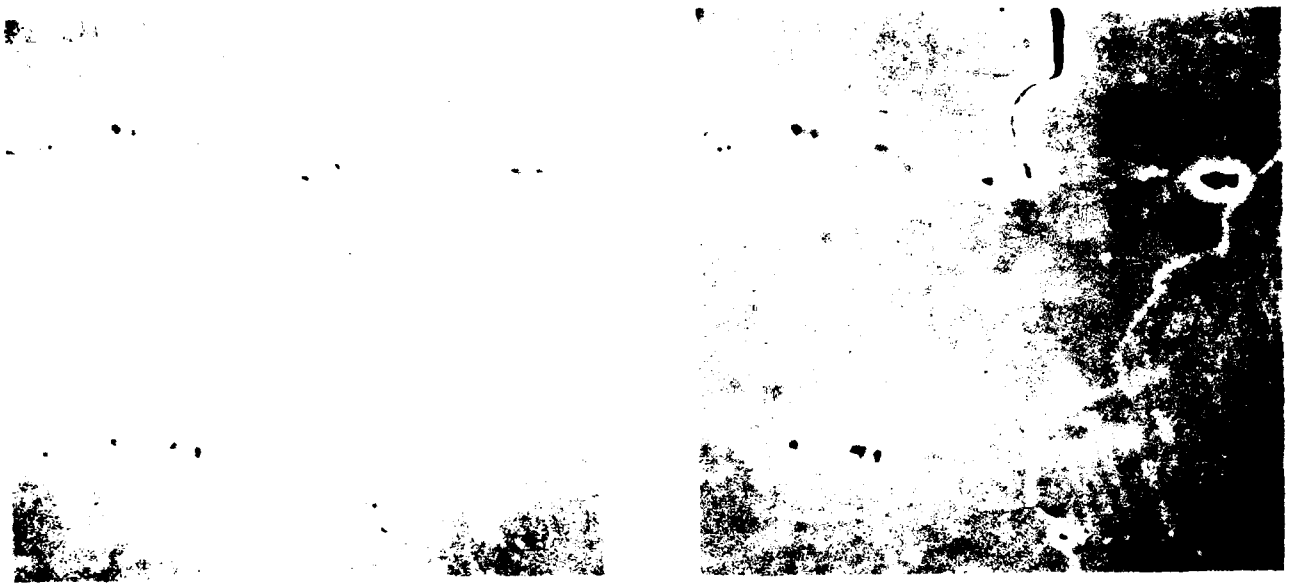

Figure 6. 7075-T6, ΔK = 10 $MN/m^{3/2}$, R = 0.25, wet air environment. Set 45.
Left: minimum load. Right: maximum load.

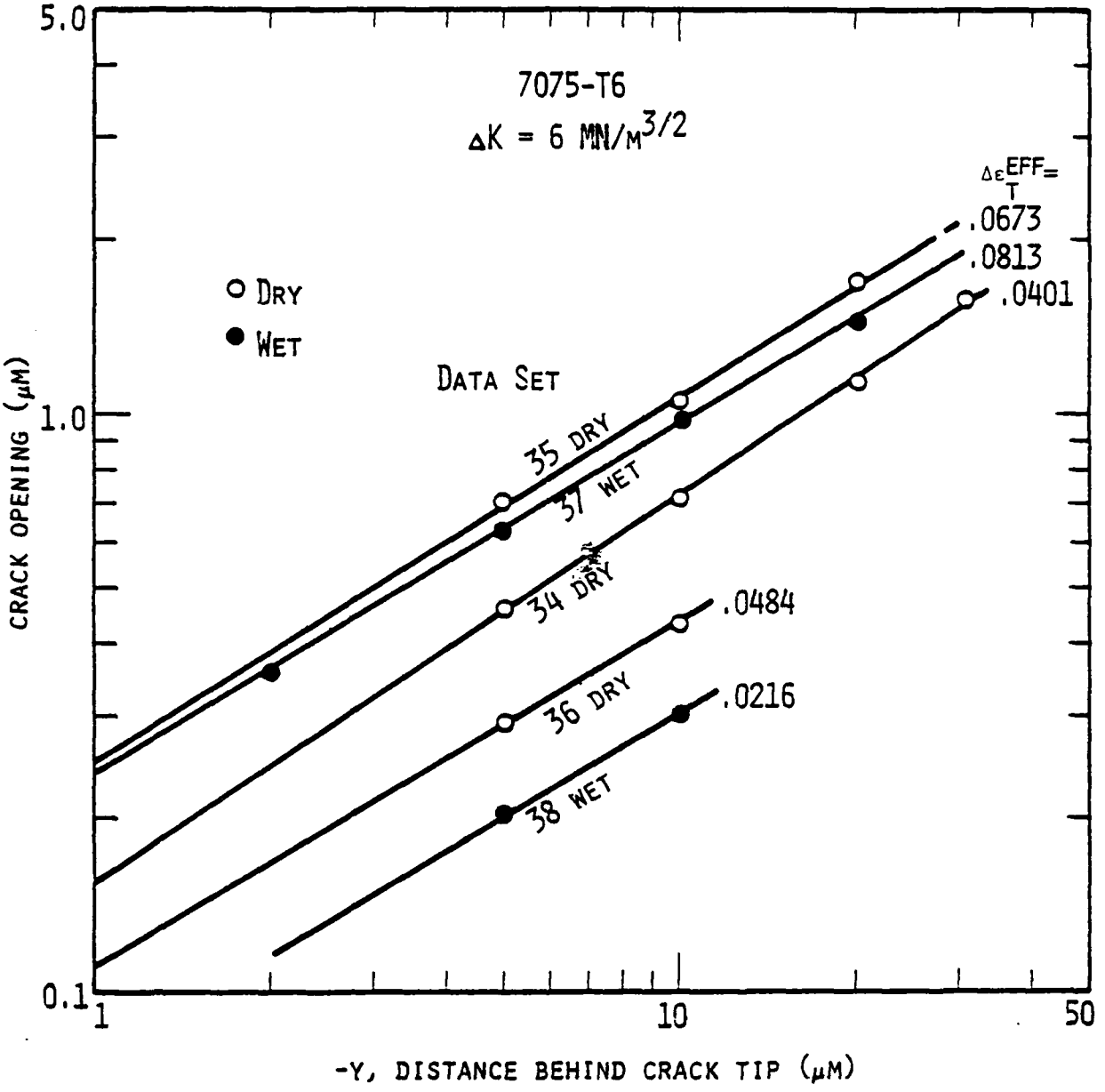

Figure 7. Crack opening vs distance behind crack tip: $\Delta K = 6$ MN/m$^{3/2}$.

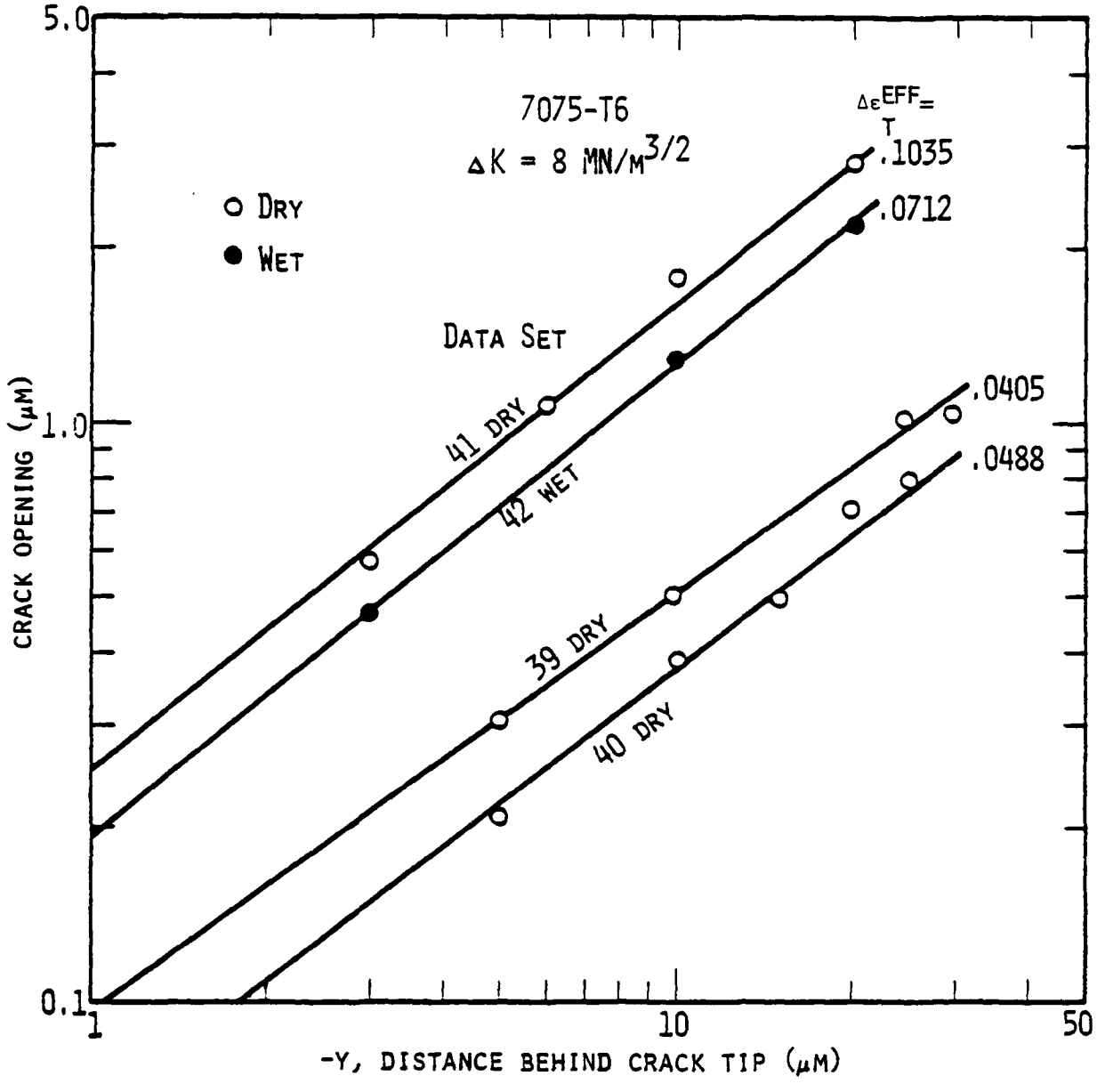

Figure 8. Crack opening vs distance behind crack tip: $\Delta K = 8$ MN/m$^{3/2}$.

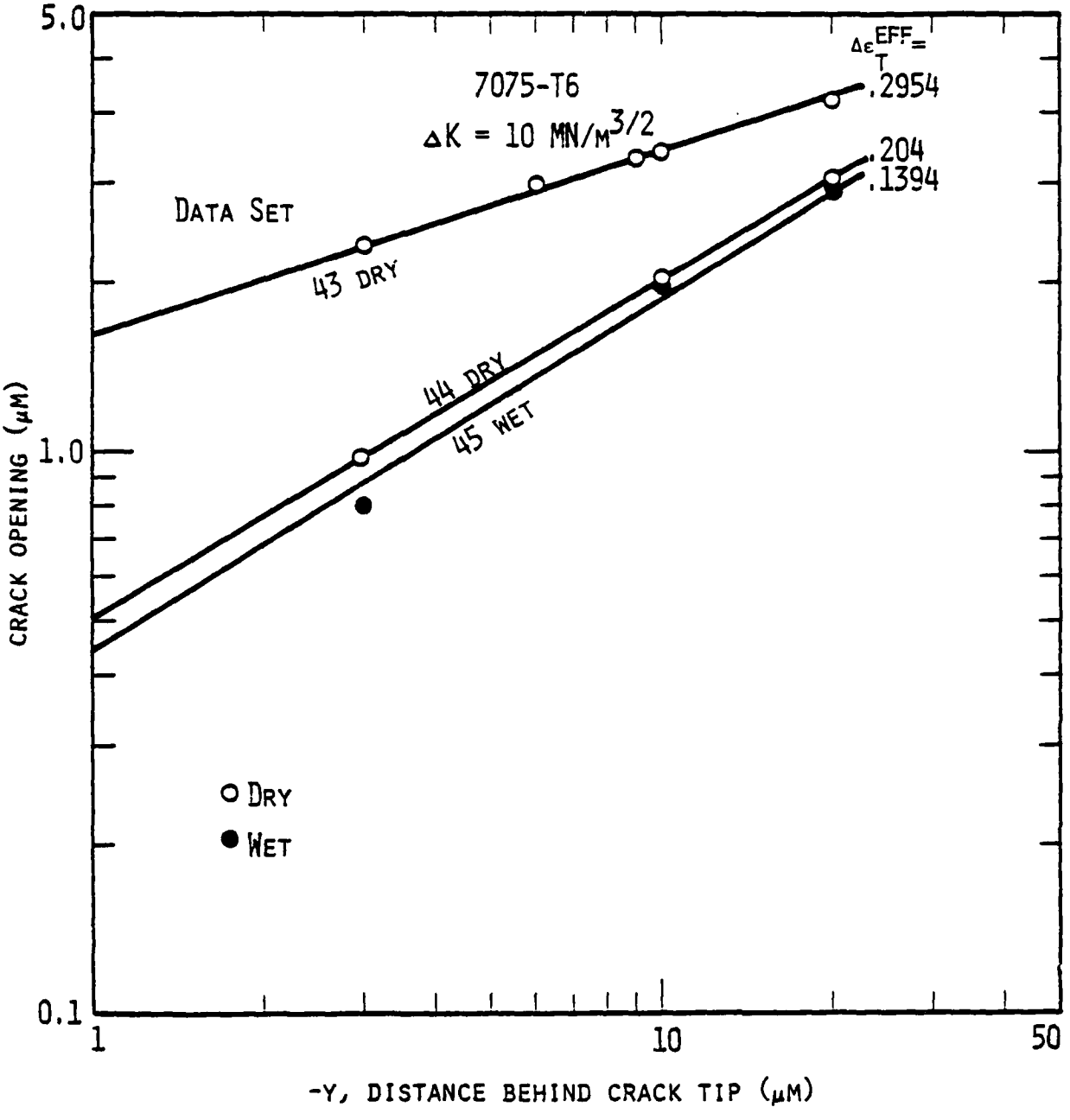

Figure 9. Crack opening vs distance behind crack tip: $\Delta K = 10\ MN/m^{3/2}$.

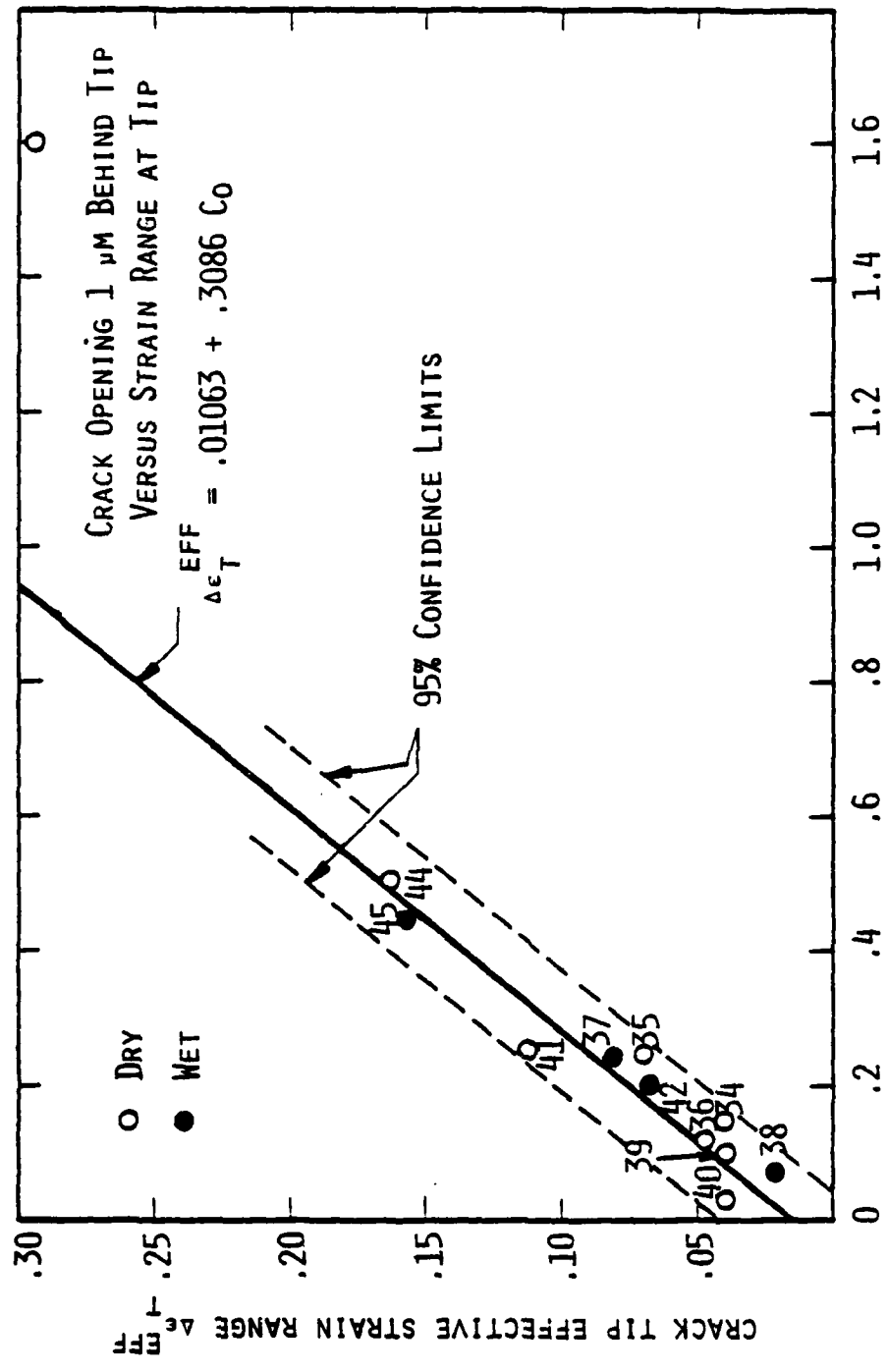

Figure 10. Total effective strain range at the crack tip vs crack opening at 1 μm behind crack tip.

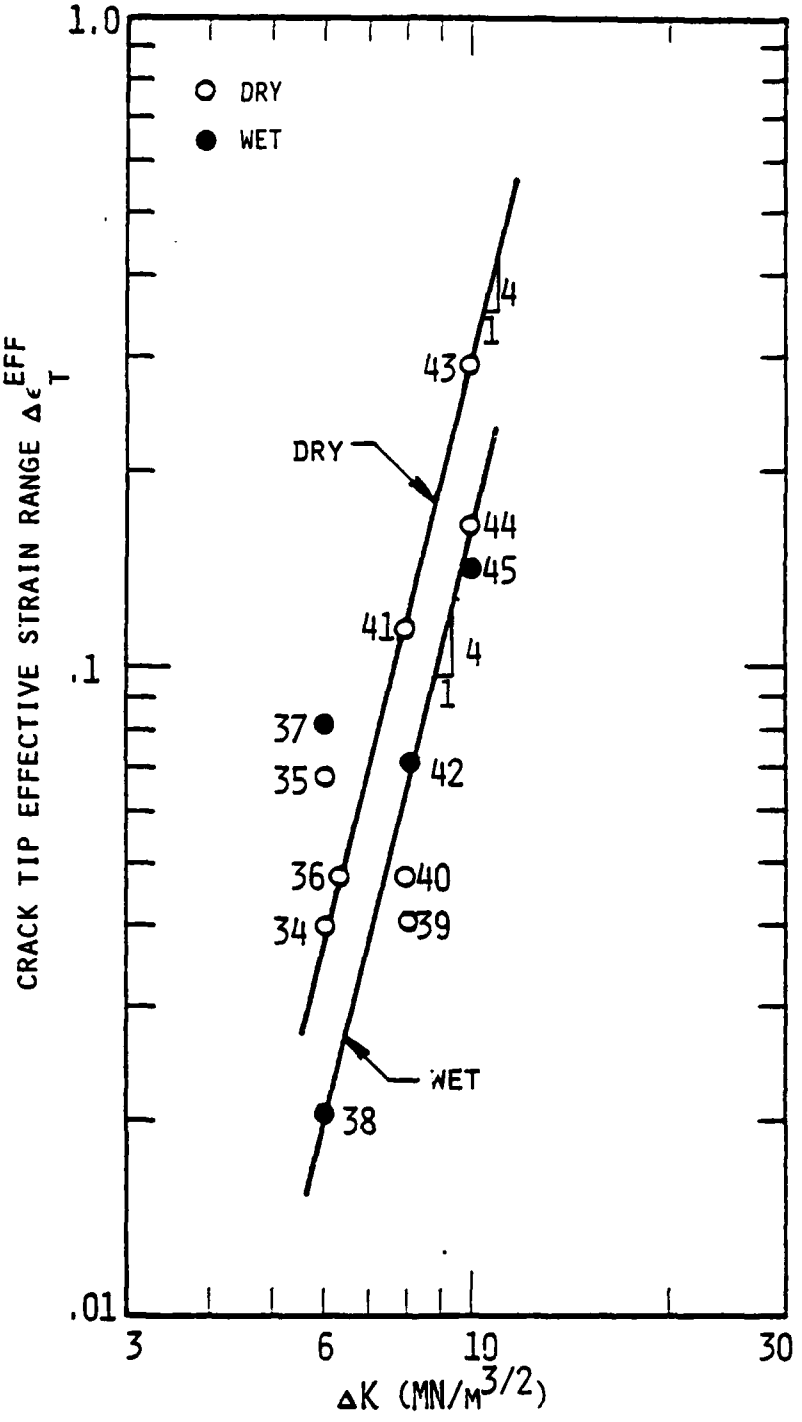

Figure 11. Total effective strain range at the crack tip vs cyclic stress intensity factor.

The data of Table I are replotted in Figure 11 to show the relation between $\Delta\varepsilon_t^{eff}(o)$ and ΔK. The considerable variation evident is considered to be due principally to the nature of the fatigue process* and not the capability to accurately measure crack tip strains. For comparison purposes, lines with a slope of 4 are drawn through the data for both environments. This has required that some of the data be ignored, and it is not known currently if this is justified.

Another very important result obtained from the data is the distribution function for the strain range within the plastic zone. The use of selected area electron channeling on aluminum alloys[14] has shown that the strain distribution has the form

$$\varepsilon_t = \varepsilon_o - m \ln(A + r) \tag{4}$$

where r is the radial distance from the crack tip in μm, and ε_t is the equivalent tensile strain, as derived by calibration using selected area electron channeling patterns from a tensile specimen. This strain, ε_t, should be related to the crack tip strain range, $\Delta\varepsilon$, as indicated by the Appendix to Ref. 14. Thus, the expected form of the strain range distribution function is

$$\Delta\varepsilon_t^{eff} = \varepsilon_o - m \ln(A + r) \tag{5}$$

as derived from the stereoimaging data. The reason for using $\Delta\varepsilon_t^{eff}$, a combination of the principal strains, is that it produces scalar, rather than vector quantities, which are easier to comprehend in the biaxial field of the crack tip. The subscript "t" refers to the total strain, i.e., the elastic + plastic strains.

If the data fits the form of Eq. (5), then it should yield a straight line by plotting $\Delta\varepsilon_t^{eff}$ vs $1/r$. Two examples are shown, Figures 12 and 13, both at $\Delta K = 10$ MN/m$^{3/2}$. At lower ΔK there is more scatter in the data. Appendix C shows plots of $\Delta\varepsilon_t^{eff}$ vs distance from the crack tip, as derived from Figures 3-6. By looking at a large quantity of data in several

---

*Dynamic high resolution observation of fatigue crack growth in the SEM has shown that crack tips do not deform the same each cycle. Even though these observations were made in vacuum, this behavior is thought to be typical of other environments as well. For a constant ΔK, there is a cycle of crack tip sharpening and blunting where the crack first grows and the crack tip is sharp, followed by tens to hundreds of cycles, depending on ΔK, during which the crack opens to successively larger magnitudes, terminating in another increment of crack growth. The data, Table I, probably reflects these variations, because no attempt was made to bias the observations by selective analysis of the collected photographs. It is the variation in crack opening during the sharp/blunt cycle which causes the corresponding variation in crack tip strain which produces a large measure of the scatter in Figure 11.

directions around the crack tip, the general validity of Eq. (5) becomes evident, even though for any one set of data there is considerable scatter. The constants in Eq. (5) for the direction ahead of the crack for all the 7075-T6 crack tips analyzed are given in the right hand portion of Table I. These values are derived by hand fits of the equation to the data, and should be considered as preliminary, which means that no specific interpretation is being made at this time. It is interesting to note, however, that if only the data on the lines in Figure 11 are considered, the slope of the equation, m, increases with increasing ΔK for both environments, and m for the dry environment is greater than for the wet environment. No similar traits are seen for the paramenter A, but these values are very sensitive to the other derived values in the equation. Considerably more working with the data could be done to derive self-consistent values of the constants; this has not yet been done because more data is required so that the final form of the information will have statistical validity.

IV. DISCUSSION OF RESULTS

The correlation derived between crack opening and distance behind the crack tip, as expressed by Eq. (3) appears, statistically, to be valid within the range of about 1 to 100 μm, and it helps to explain the wide variation in crack tip strains evident in Figure 11, through the correlation found in Figure 10 (recall footnote, p. 17). By relating crack opening at 1 μm behind the crack tip to the crack tip strain range a fairly good correlation is obtained, except for the largest strain obtained.

The relationship expressed by Equation (3) may be more than empirical. Amazigo and Hutchinson[15] have determined analytically the crack tip singularity fields for a steadily growing crack in a linear strain hardening material, and although the analysis is for non-cyclic loading, it might be relevant to the steady-growing, cyclic situation under consideration. In particular, it is predicted that the crack opening displacement behind the crack tip should be

$$C = C_o|-y|^{s+1} \tag{6}$$

where C_o is a constant, and s is dependent upon the strain hardening parameter α*. For 7075-T6 α is approximately 0.1, which in turn implies $s \simeq -0.2$. Insertion of this value into Equation (6) yields a theoretical crack opening relationship of the form

$$C = C_o|-y|^{.8} \tag{7}$$

As shown in Table I, the experimentally determined exponent for the distance term in Equation (3) averages about 0.7 for both wet and dry environments, in excellent agreement with the theoretical prediction. Since the latter implicitly ignores any environmental effect, the implication of the experimental

---

*α is defined as the ratio of the tangent modulus in the linear hardening plastic portion of the stress-strain curve, to the elastic modulus.

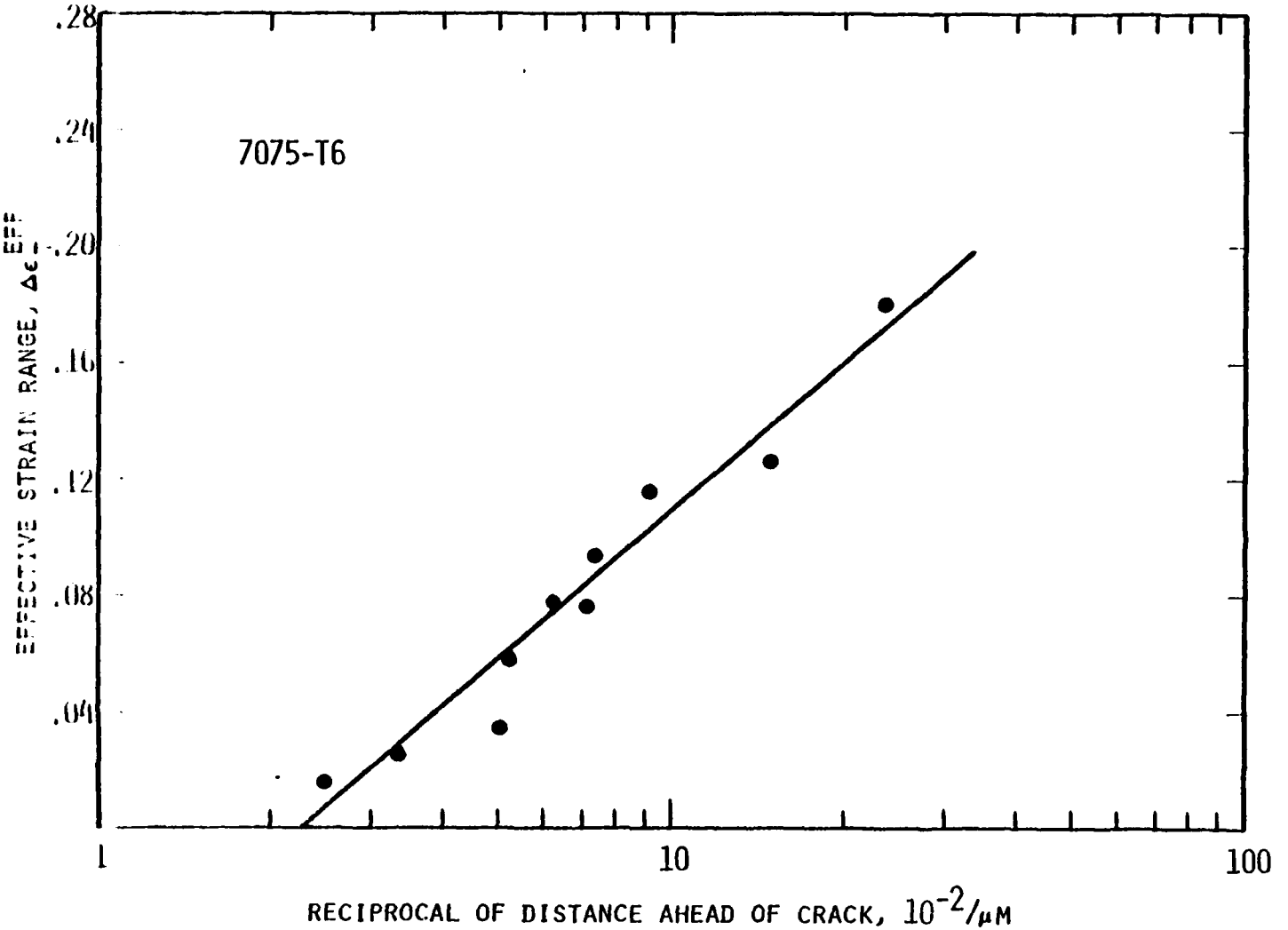

Figure 12. Total effective strain range vs reciprocal of distance ahead of crack tip: ΔK = 10 $MN/m^{3/2}$, R = 0.25, vacuum environment. Set 43.

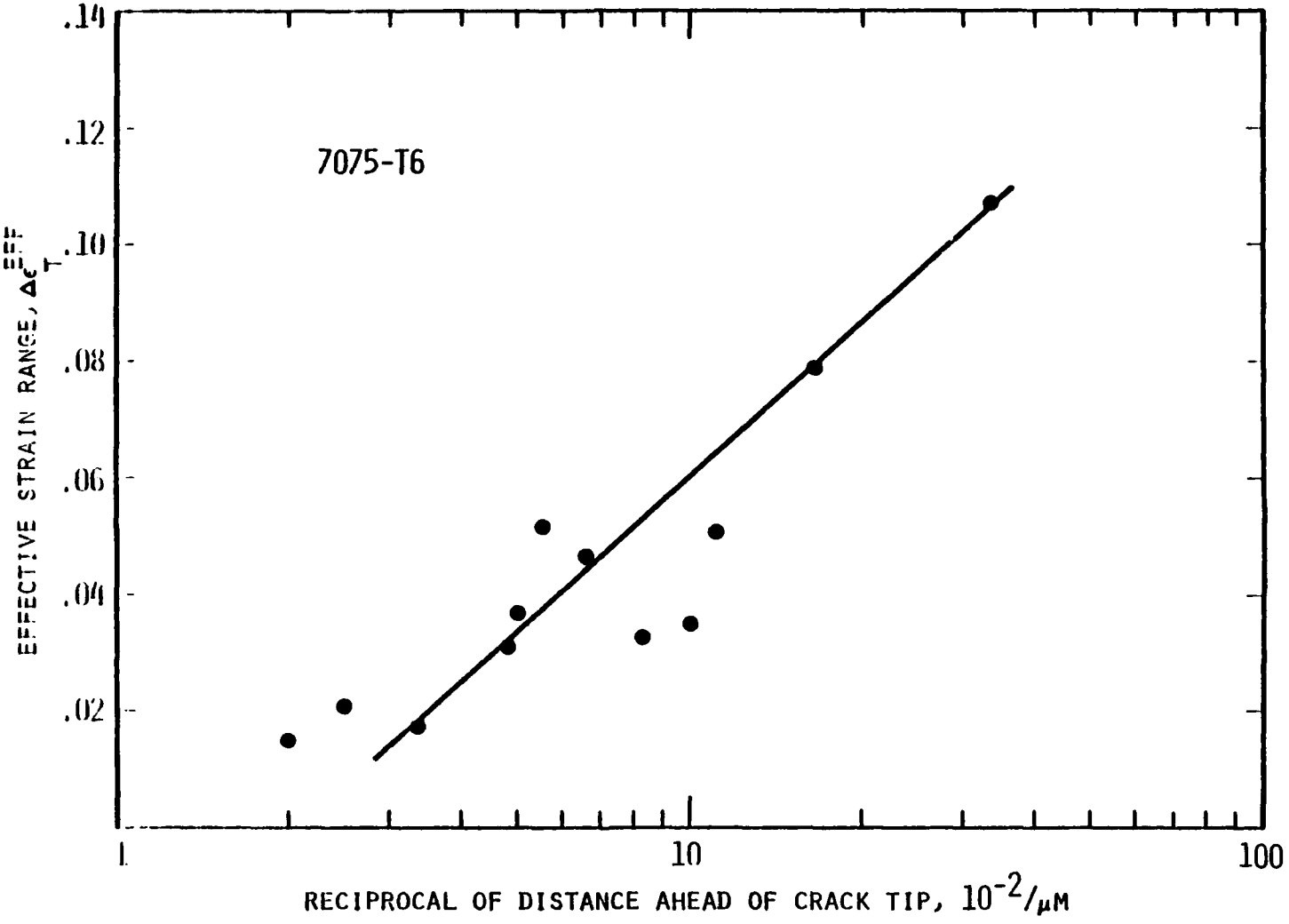

Figure 13. Total effective strain range vs reciprocal of distance ahead of crack tip: $\Delta K = 10$ MN/m$^{3/2}$, $R = 0.25$, wet air environment. Set 45.

results is that crack tip strain hardening may be essentially unaffected by the environment. This would contradict the microhardness test results[3] described earlier.

The thickness of the specimens observed here is 3mm, and the plastic zone sizes are about 200 μm,[14] as measured by selected area electron channeling. Thus, the ratio of thickness to plastic zone size is 15. The constraints are, therefore, sufficient to expect conditions of plane strain to be prevalent near the crack tip, while right at the crack tip, this condition is considerably lessened, particularly when the strains are large. It is this last factor which may account for the disparity between the crack opening and crack tip strain of data set 43; the crack tip deformation mode may be changing from predominantly plane strain to plane stress in this case.

It does appear (Figure 11) that there is a tendency for local crack tip strain ($\Delta\varepsilon_t^{eff}$) to be larger in dry environments, in agreement with metallographic observations and fractographic interpretations described earlier. It is not known as yet, however, whether this effect persists to strains further out in the plastic zone. Our earlier work on low carbon steel[16] did demonstrate higher strain in dry (versus wet) throughout the plastic zone, to the extent the plastic zone boundary in a dry environment exceeded that in an agressive one. Experiments in progress will address this issue for aluminum alloys.

The correlation between crack tip strain range and crack opening, Figure 10, and between crack tip strain range and ΔK, Figure 11, both indicate an interesting fact: for a crack opening of zero, a finite crack tip strain is required, approximately $\Delta\varepsilon^{eff} = 0.01$. For this value of strain a stress intensity of 4.3 $MN/m^{3/2}$ would be required (Figure 11). If 7075-T6 had a sharp yield point, 0.01 is approximately the strain range which would correspond to the stress range at yield; 7075-T6 does not have a sharp yield point, however. No reliable data is available for the threshold stress intensity for 7075-T6 in an inert environment, but $\Delta K_{TH} = 4.3$ $MN/m^{3/2}$ is a reasonable value for the expected value (which is dependent on how it is defined). For the wet environment, a crack tip strain of 0.01 would be expected at $\Delta K = 5$ $MN/m^{3/2}$, compared to measured values of about $\Delta K = 2.5$ $MN/m^{3/2}$ at $R = 0.1$. This apparent inconsistency may be partially explained by the fact that crack growth rates in the wet environment are approximately twice those in the dry environment. To attain the same growth rate, thereby defining ΔK threshold for the wet environment, the stress intensity factor must roughly be one half that for the dry environment, or 2.1 $MN/m^{3/2}$. This would imply that crack tip strain range of roughly one half yield values would pertain at the crack tip near ΔK threshold.

By interpreting the data as is done in the preceeding paragraphs, the effect of environment on fatigue crack growth in 7075-T6 is inferred as being much the same as in low carbon steel; namely, faster crack growth occurs because the environment lowers the strain which may be sustained at the crack tip, and hydrogen is the most likely specie in the environment for the cause of such an effect. The other issues related to these environmentally induced changes in crack tip plasticity are still being investigated.

V. SUMMARY AND CONCLUSIONS

Crack tip plasticity parameters have been measured for 7075-T6 aluminum alloy in a wet environment (100% RH) and a dry environment (10^{-5} torr vacuum) using the stereoimaging technique. The following summarizes the results and conclusions to date:

1) Crack opening behind the crack tip is a power function of distance from the tip.

2) Crack tip strain range correlates well with crack opening one micrometer behind the crack tip.

3) Considerable variation occurs in crack tip strain range and crack opening displacement for a fixed value of cyclic stress intensity factor. This scatter is considered to be typical of fatigue crack growth, and not a consequence of the measurement technique.

4) Crack tip strains are found to be dependent on ΔK^4 for both wet and dry environments. Threshold ΔK in the dry environment may be related to elastic strain range at the crack tip.

5) The wet environment may be thought of as allowing increased fatigue crack growth by decreasing the strain which may be supported at the crack tip.

REFERENCES

1. P. E. Irving and L. N. McCartney, Met. Sci., 1977, 351.

2. B. I. Verkin and N. M. Grinberg, Mat. Sci. Eng., 41, 1979, 149.

3. B. Bouchet and J. de Fouguet, Proc. 4th Int. Conf. on the Strength of Metals and Alloys, Nancy, 1976, 485.

4. B. Bouchet, J. de Fouguet and M. Aguillon, Acta Met., 23, 1975, 1325.

5. M. Bohmer and D. Munz, Z. Metallkd, 66, 1975, 333.

6. N. M. Grinberg, I. L. Ostapenko, and V. A. Serdyuk, Probl. Prochn. (in press).

7. L. B. Vogelsang and J. Schijve, "Environmental Effects on Fatigue Fracture Mode Transitions Observed in Aluminum Alloy," Delft University of Technology Report LR-289, November 1979.

8. E. P. Louwaard, "Effect of a Reduced Ductility at Low Temperatures on Fatigue Crack Growth in 7075-T6 Sheet Material Tested in Vacuum," Delft University of Technology Report LR-243, January 1977.

9. H. L. Ewalds, Eng. Frac. Mech., 13, 1980, 1001.

10. J. Schijve and W. J. Arkema, "Crack Closure and the Environmental Effect on Fatigue Crack Growth," Delft University of Technology Technical Report VTH-217, April, 1976.

11. D. L. Davidson and A. Nagy, "A Low Frequency Cyclic Loading Stage for the SEM," Journal of Physics E v.11 207-210 (1978).

12. D. L. Davidson, "The Observation and Measurement of Displacements and Strain by Stereoimaging," Scanning Electron Microscopy/1979/II, p. 79-86.

13. D. R. Williams, D. L. Davidson, and J. Lankford, "Fatigue-Crack-Tip Plastic Strains by the Stereoimaging Technique," Experimental Mechanics 20, 1980, pp. 134-139.

14. D. L. Davidson and J. Lankford, "Fatigue Crack Tip Plastic Strain in High-Strength Aluminum Alloys," Fatigue of Engineering Materials and Structures, v. 3(4) 289-303 (1980).

15. J. C. Amazigo and J. W. Hutchinson, Jour. Mech. Phys. Solids, 25, 1977, 81.

16. D. L. Davidson and J. Lankford, "The Effect of Water Vapor on Fatigue Crack Tip Stress and Strain Range Distribution and The Energy Required for Crack Propagation in Low-Carbon Steel," International Journal of Fracture (in press) 1981, and ONR Annual Reports for previous years.

APPENDICES

APPENDIX A - DISPLACEMENT DIAGRAMS

APPENDIX B - MOHR'S CIRCLES OF STRAIN

APPENDIX C - EFFECTIVE STRAIN RANGE VS DISTANCE FROM CRACK TIP AHEAD OF CRACK

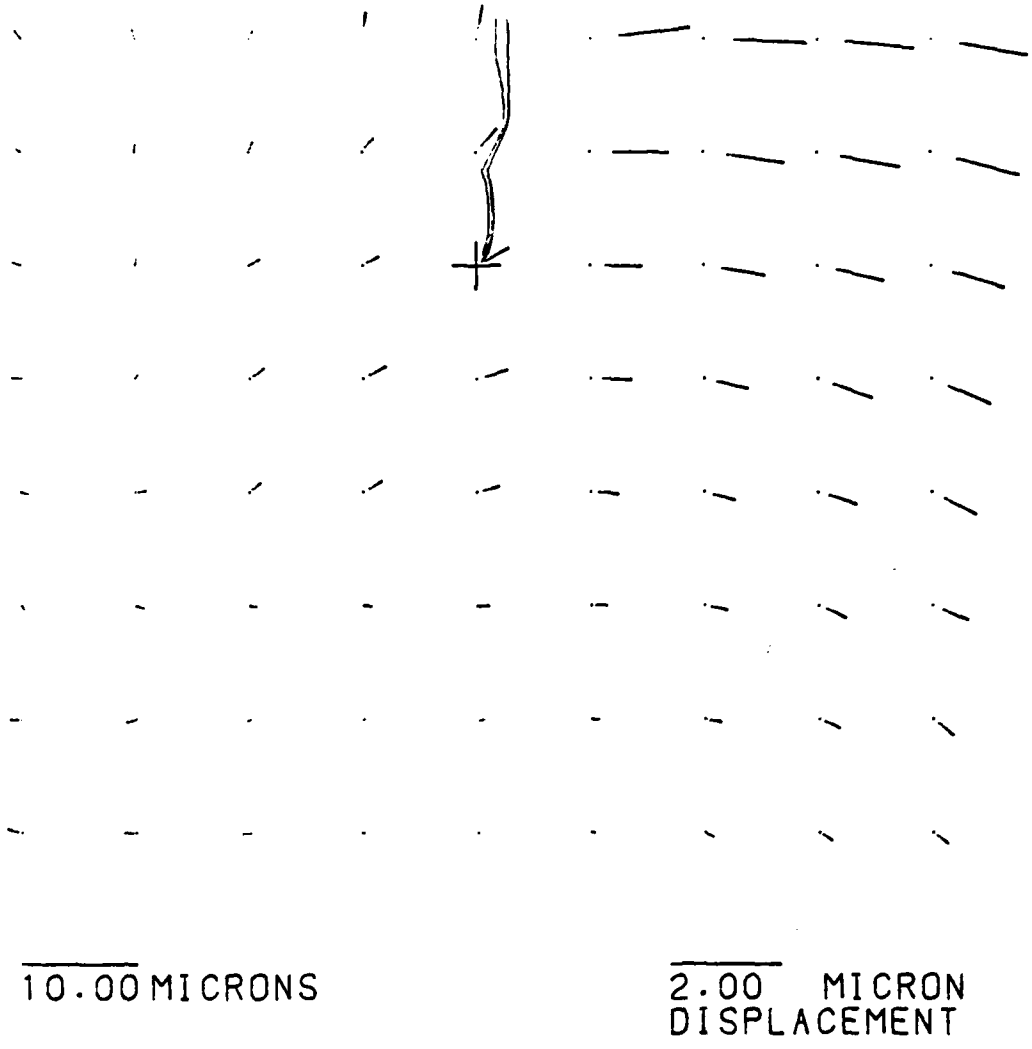

(a) Coarse grid.

Figure A1. Displacement diagram for Fig. 3. Set 35.

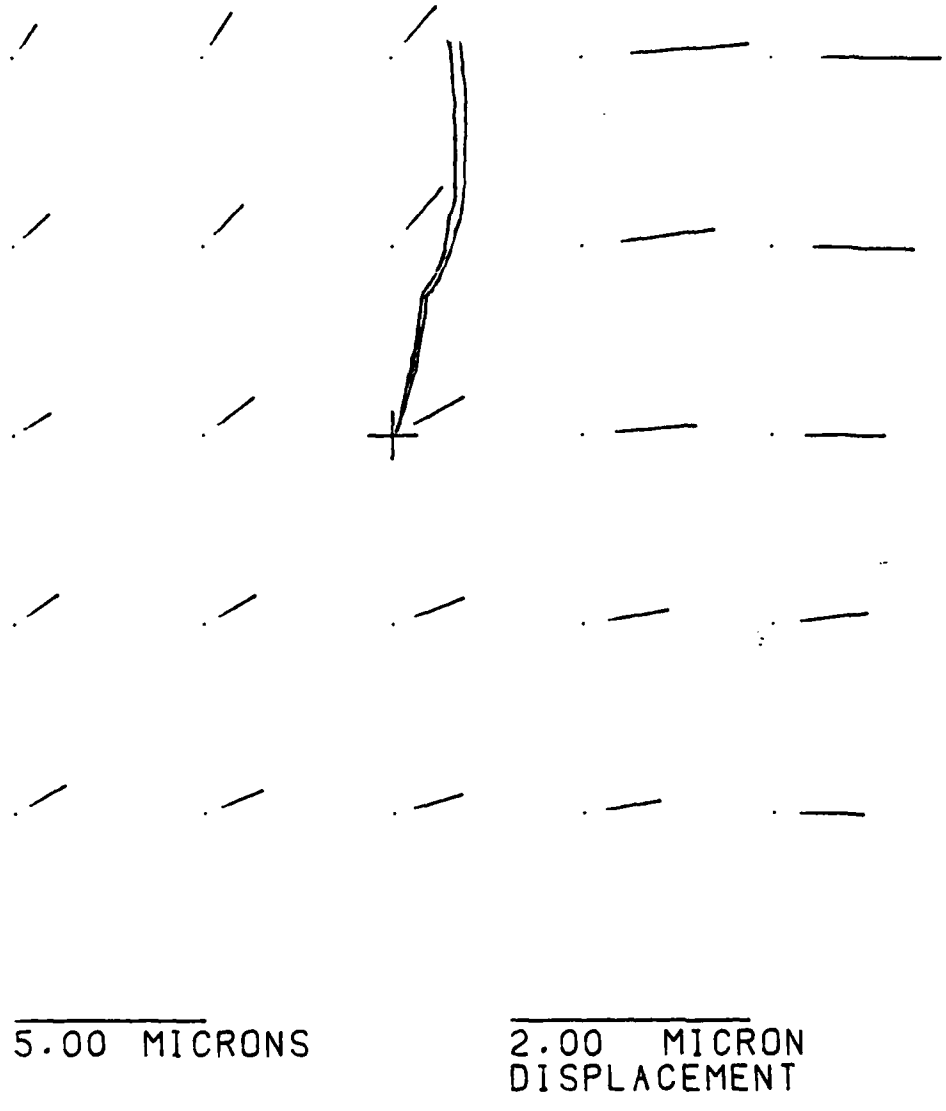

(b) Fine grid.

Figure A1 (continued). Displacement diagram for Fig. 3. Set 35.

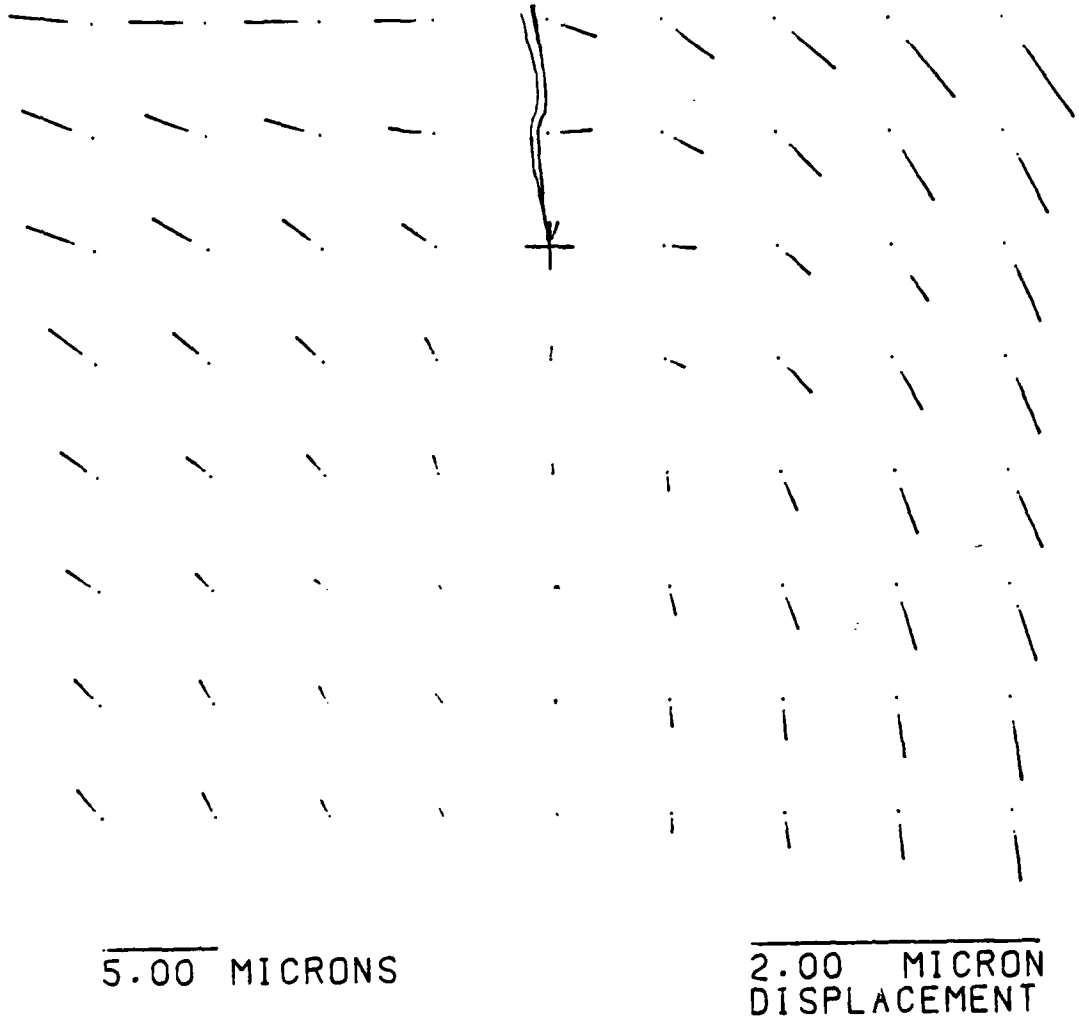

(a) Coarse grid.

Figure A2. Displacement diagram for Fig. 4. Set 37.

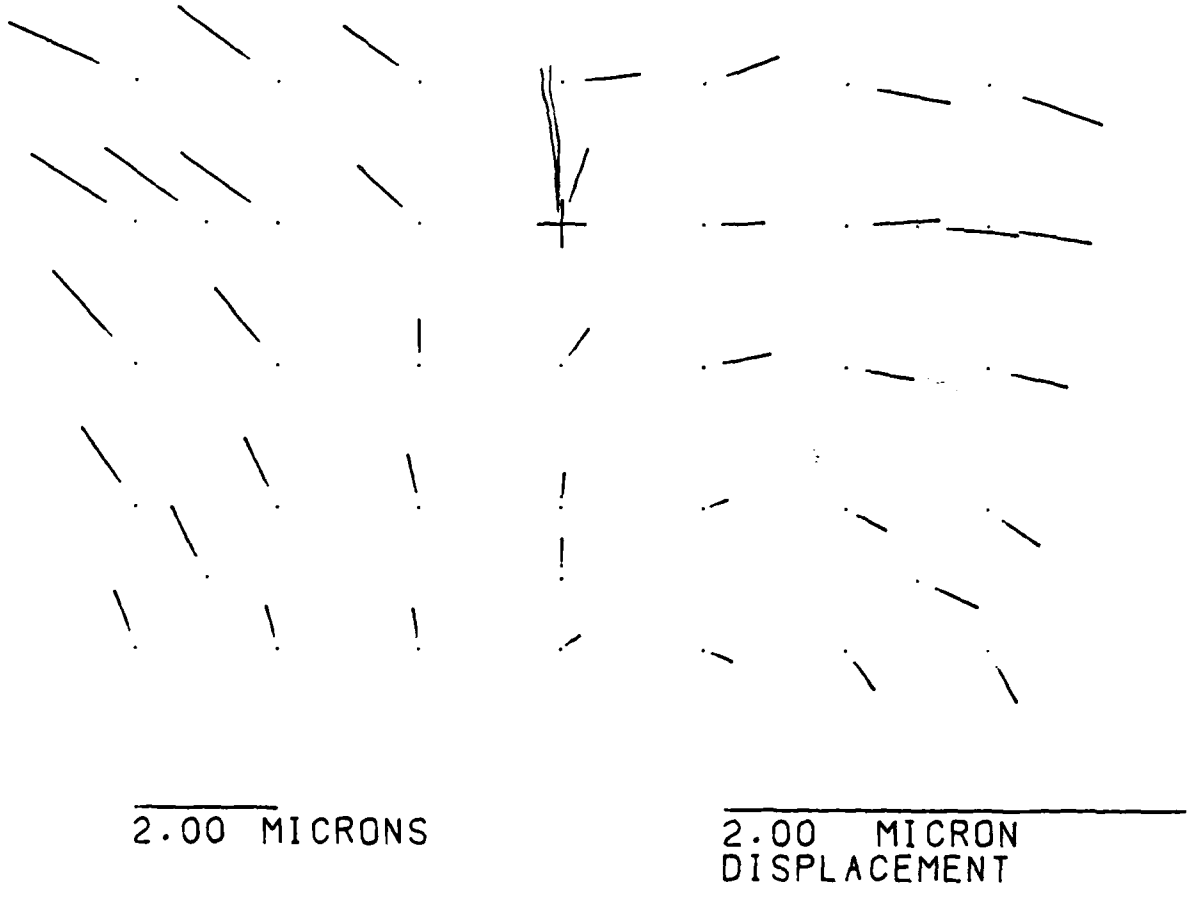

(b) Fine grid.

Figure A2 (continued). Displacement diagram for Fig. 4. Set 37.

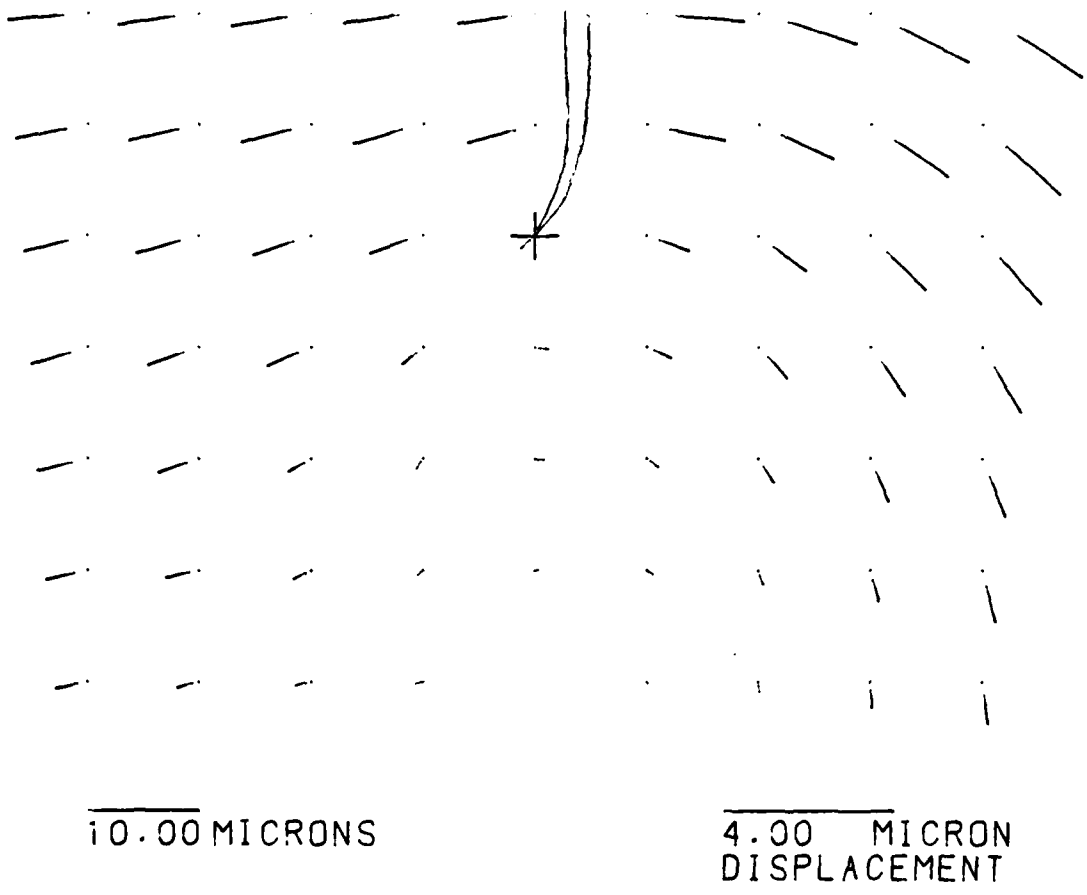

(a) Coarse grid.

Figure A3. Displacement diagram for Fig. 5. Set 43.

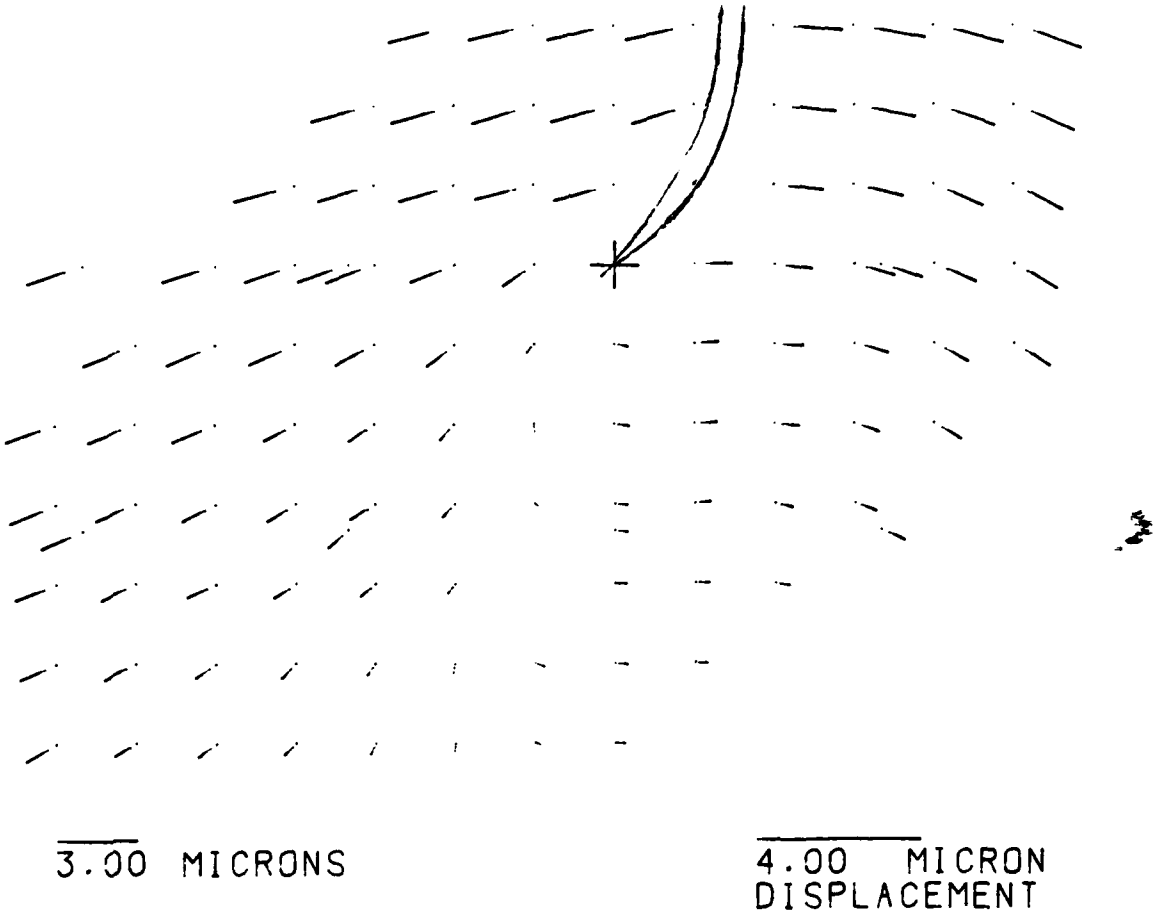

(b) Fine grid.

Figure A3 (continued). Displacement diagram for Fig. 5. Set 43.

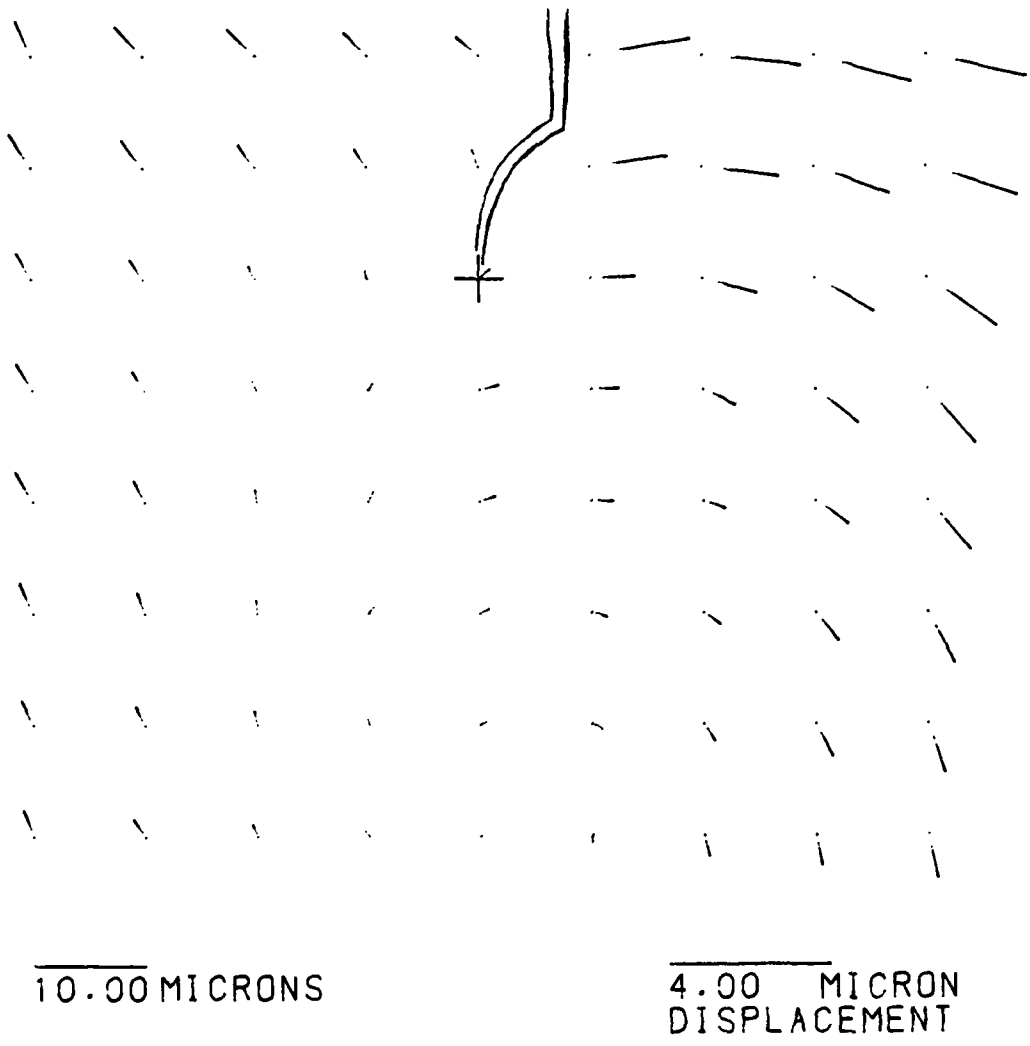

(a) Coarse grid.

Figure A4. Displacement diagram for Fig. 6. Set 45.

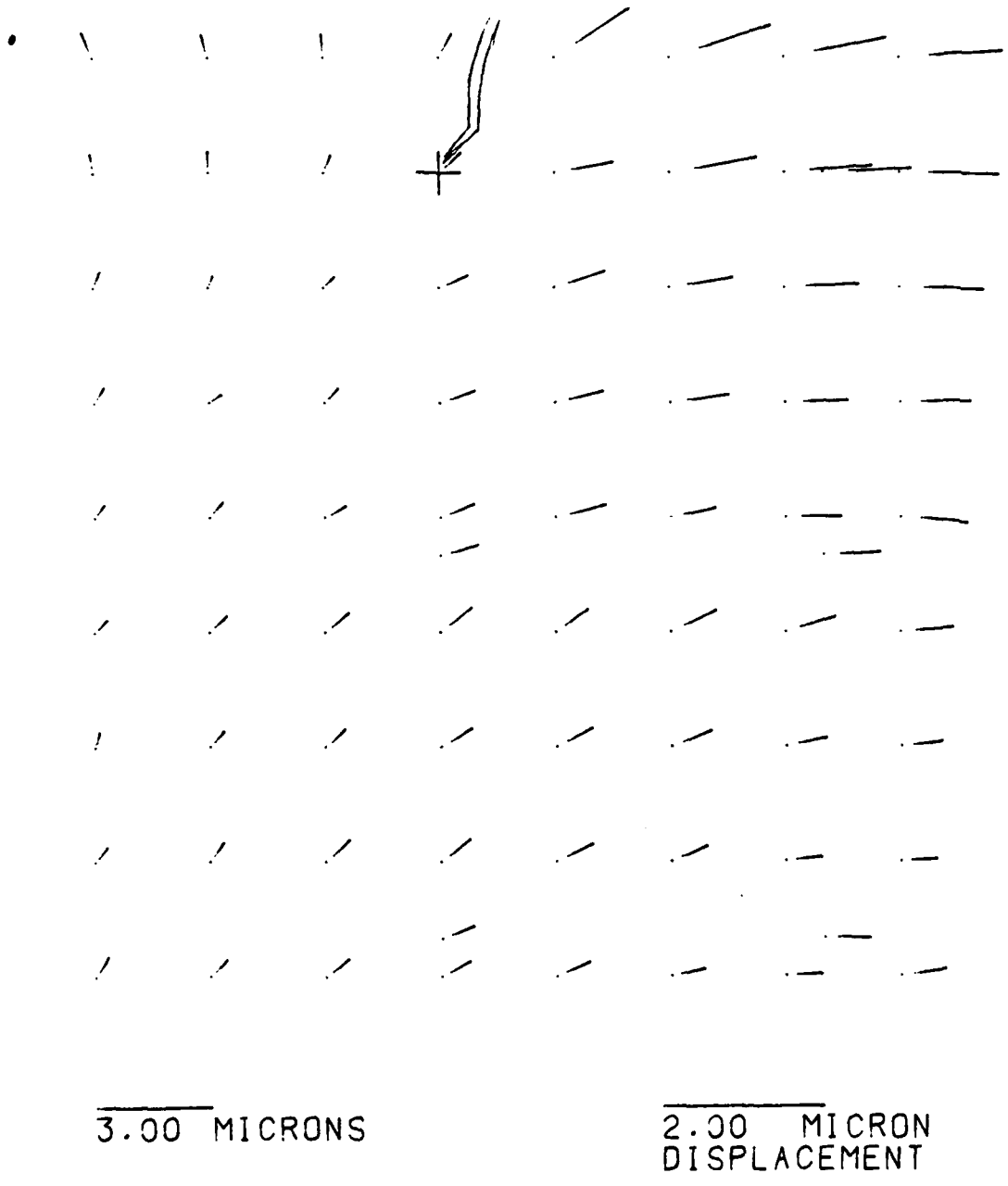

(b) Fine grid.

Figure A4 (continued). Displacement diagram for Fig. 6. Set 45.

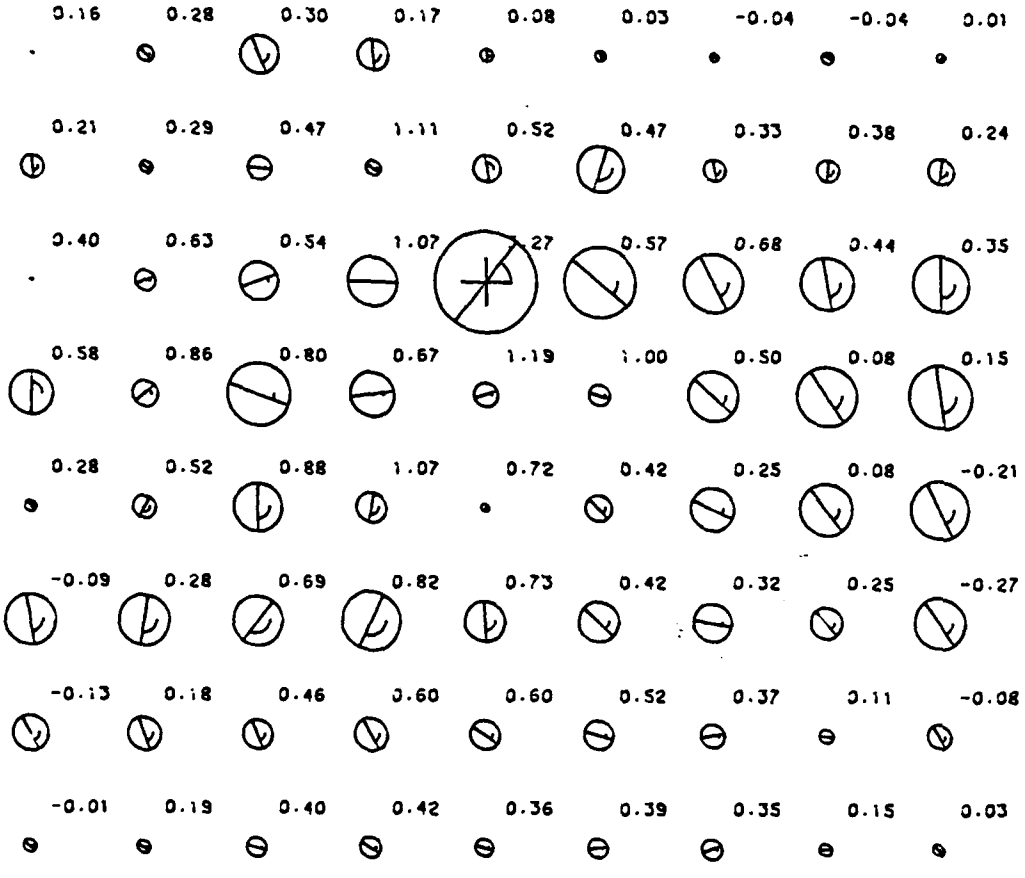

(a) Coarse grid.

Figure B1. Mohr's circles of strain, Fig. 3. Set 35.

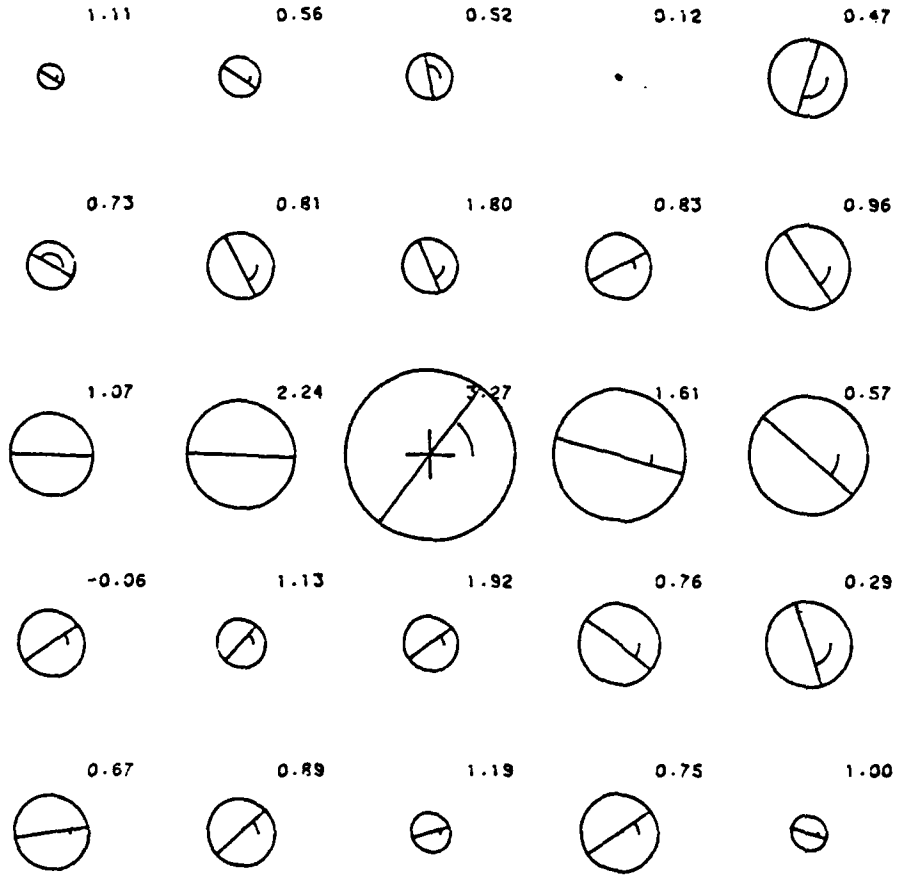

(b) Fine grid.

Figure B1 (continued). Mohr's circles of strain, Fig. 3. Set 35.

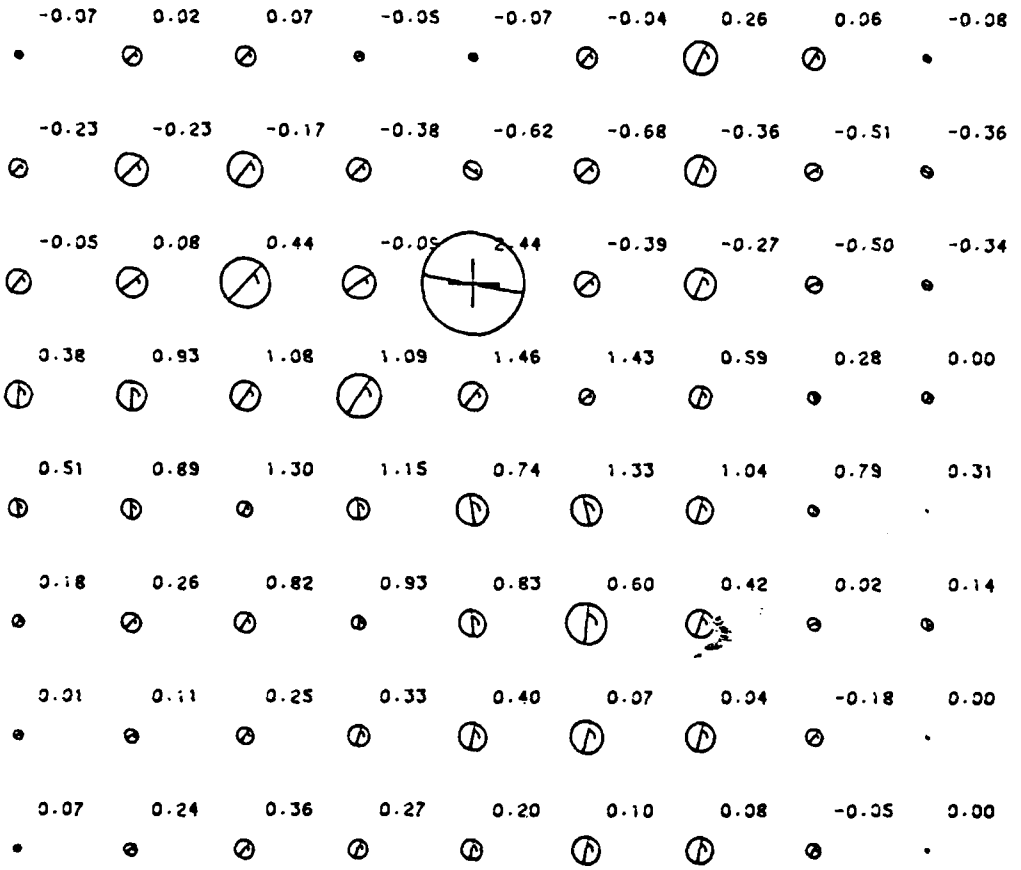

(a) Coarse grid.

Figure B2. Mohr's circles of strain, Fig. 4. Set 37.

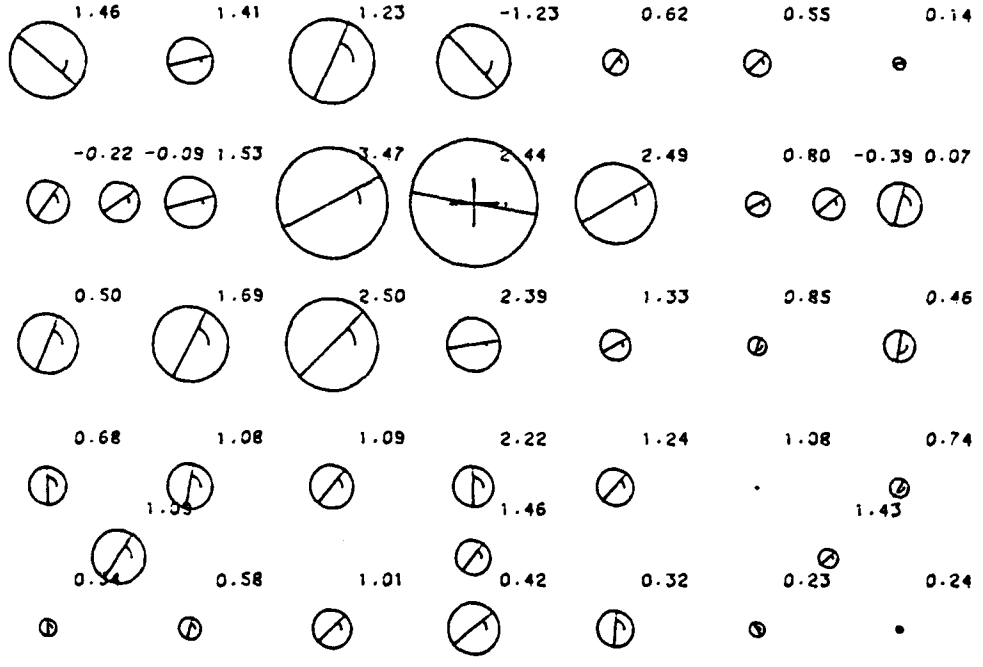

(b) Fine grid.

Figure B2 (continued). Mohr's circles of strain, Fig. 4. Set 37.

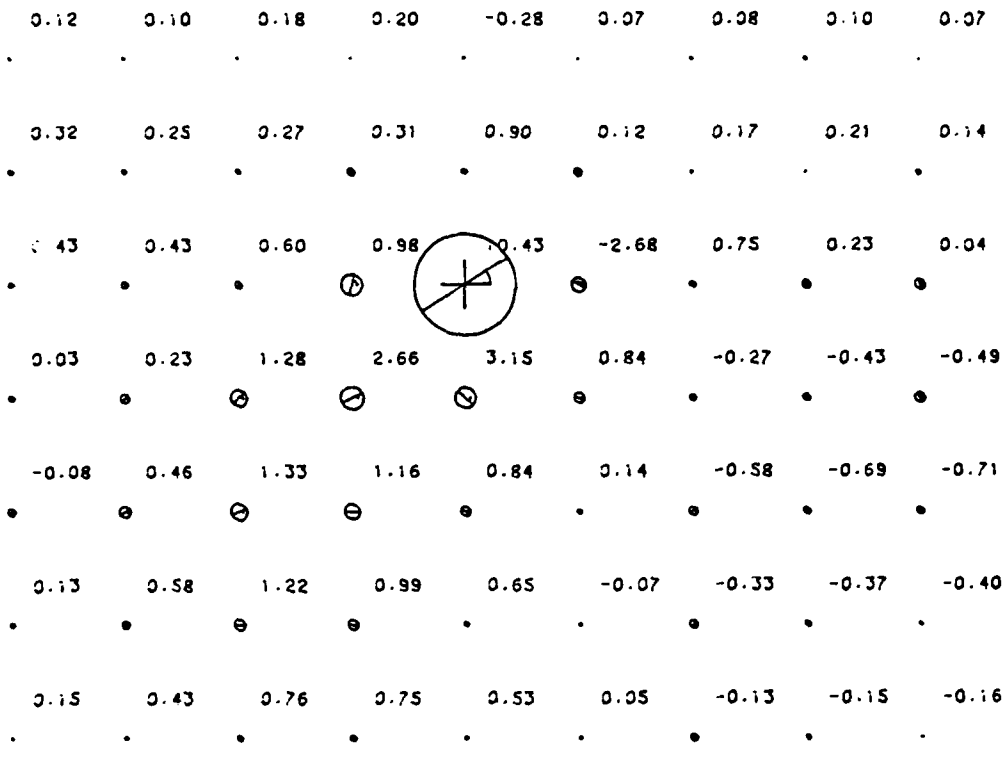

(a) Coarse grid.

Figure B3. Mohr's circles of strain, Fig. 5. Set 43.

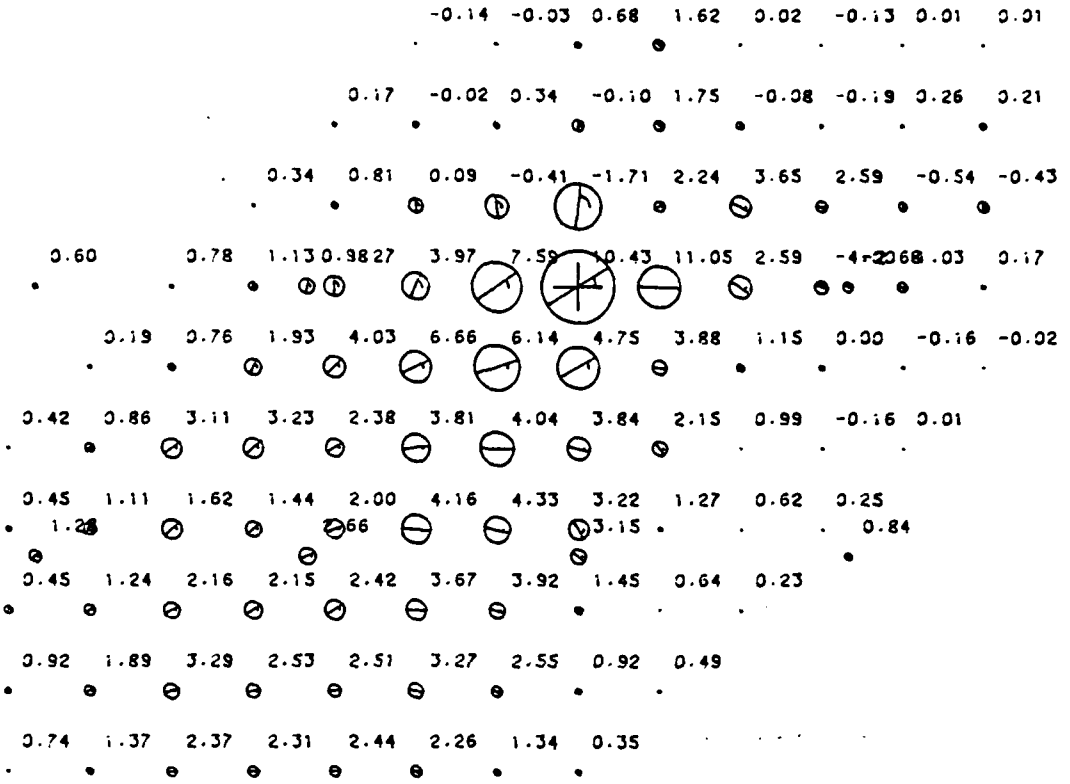

(b) Fine grid.

Figure B3 (continued). Mohr's circles of strain, Fig. 5. Set 43.

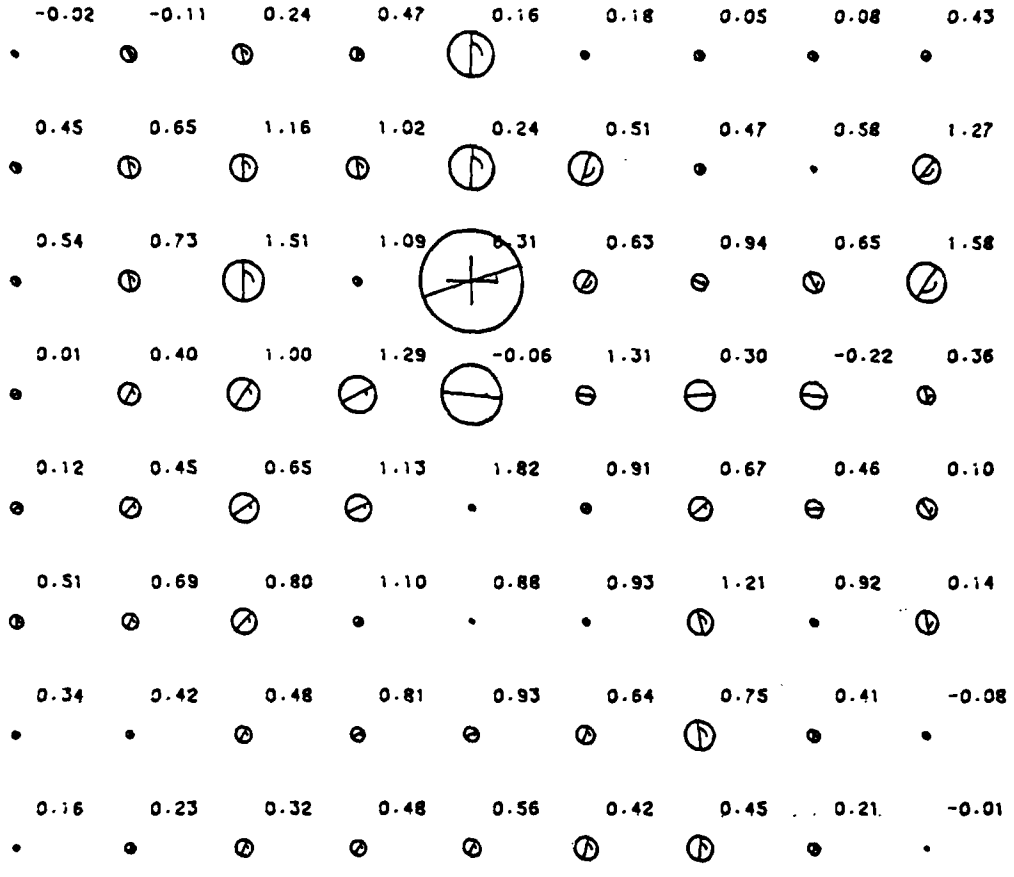

(a) Coarse grid.

Figure B4. Mohr's circles of strain, Fig. 6. Set 45.

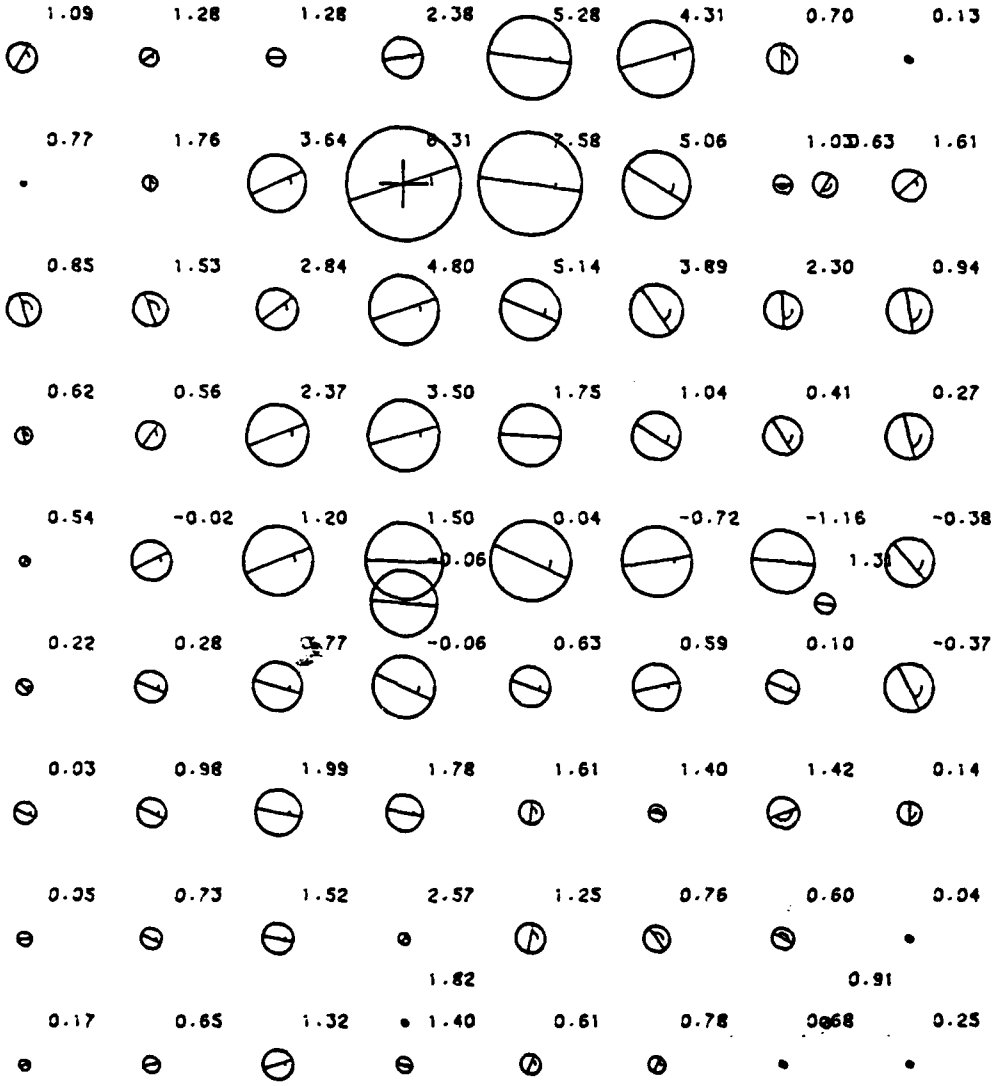

(b) Fine grid.

Figure B4 (continued). Mohr's circles of strain, Fig. 6. Set 45.

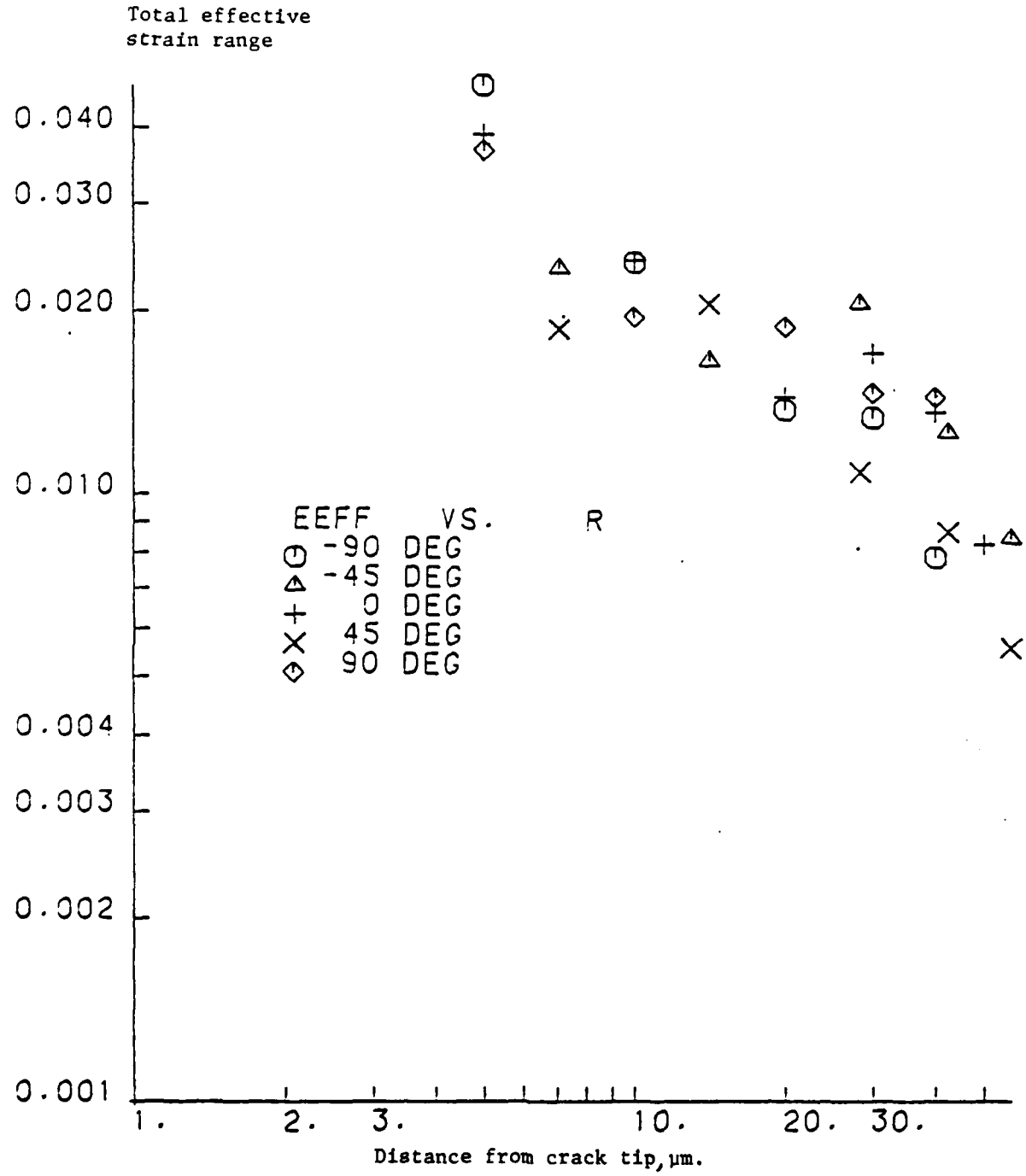

Figure C1. Total effective strain range vs distance from crack tip, Set 35.

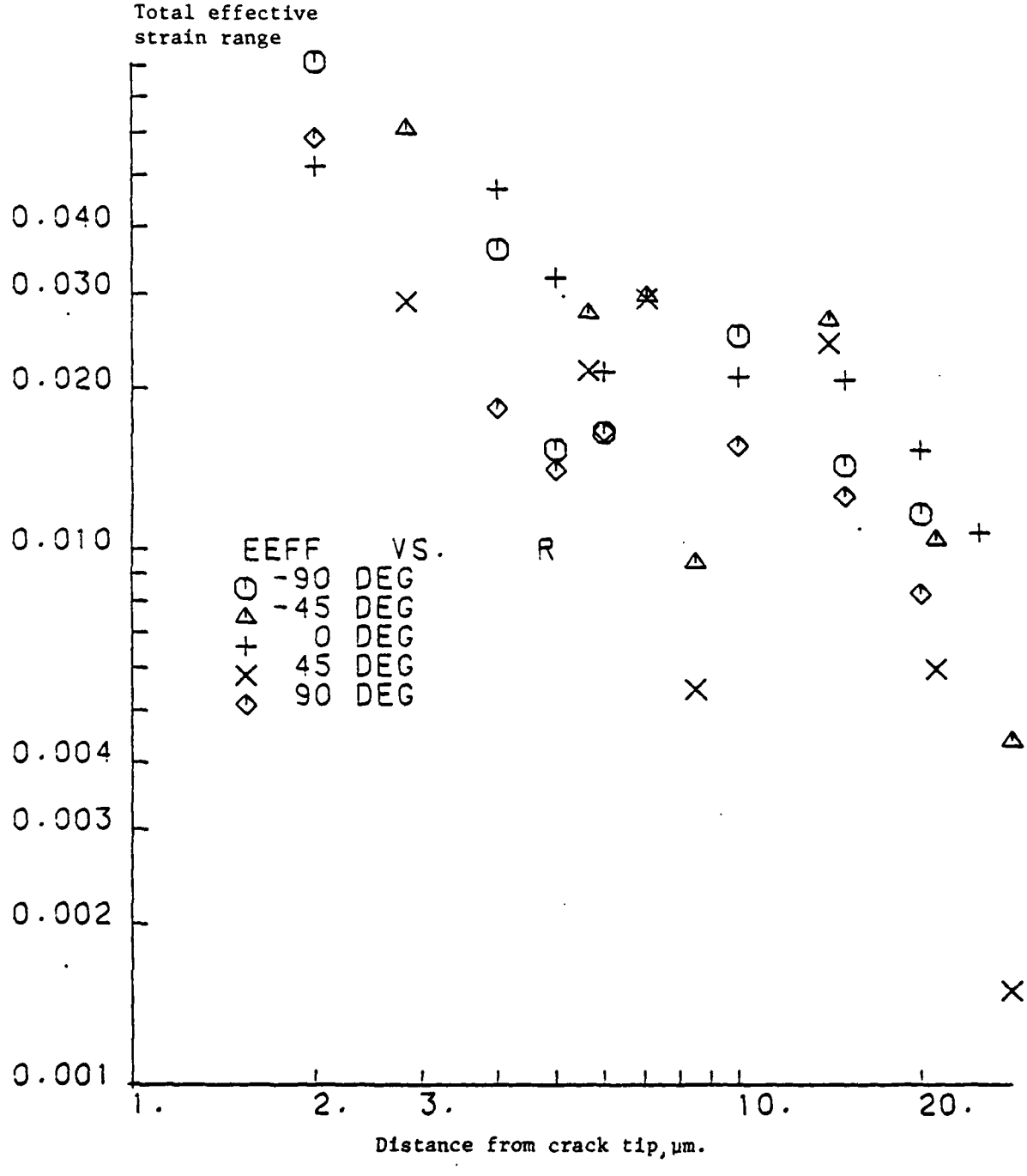

Figure C2. Total effective strain range vs distance from crack tip, Set 37.

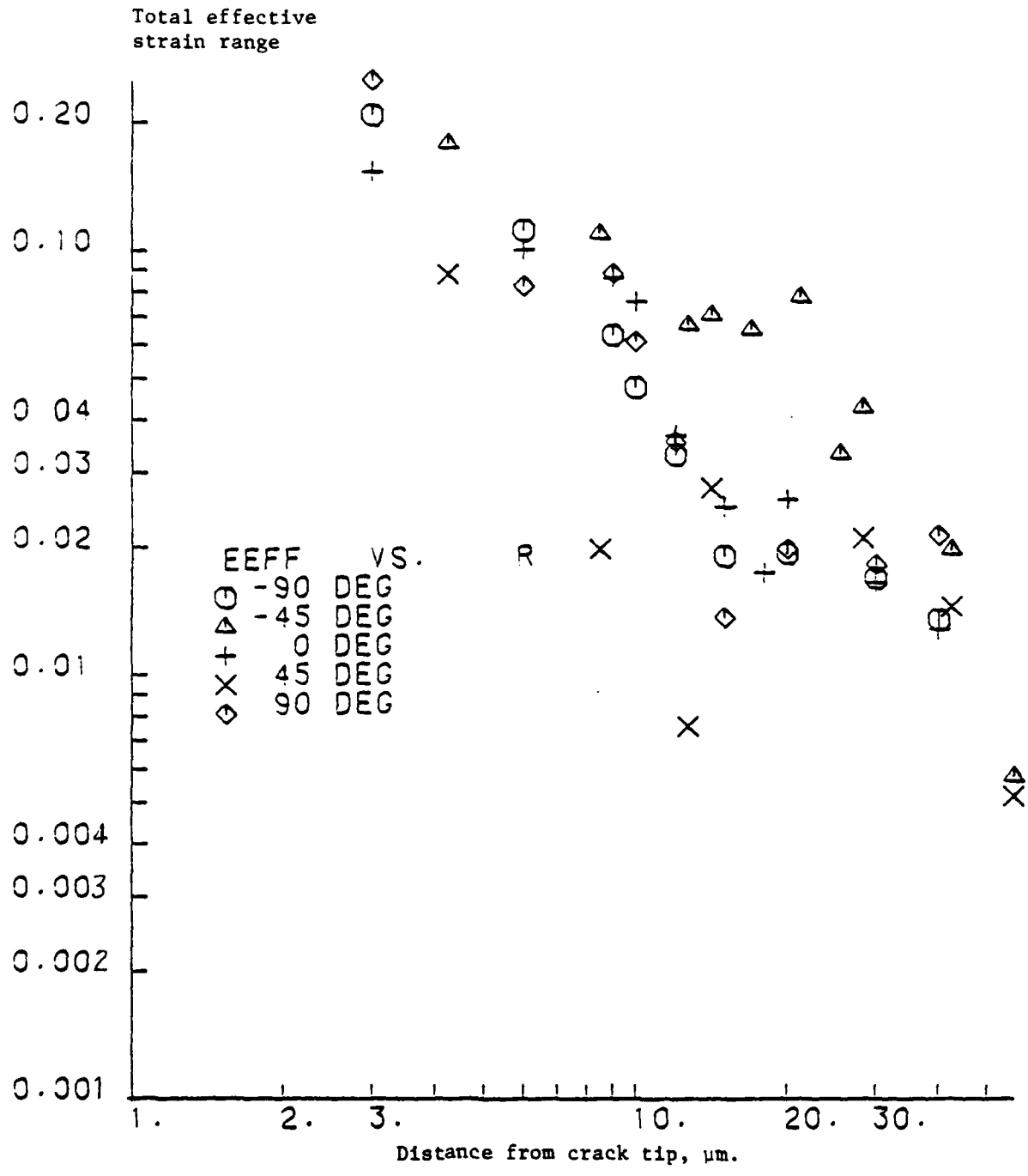

Figure C3. Total effective strain range vs distance from crack tip, Set 43.

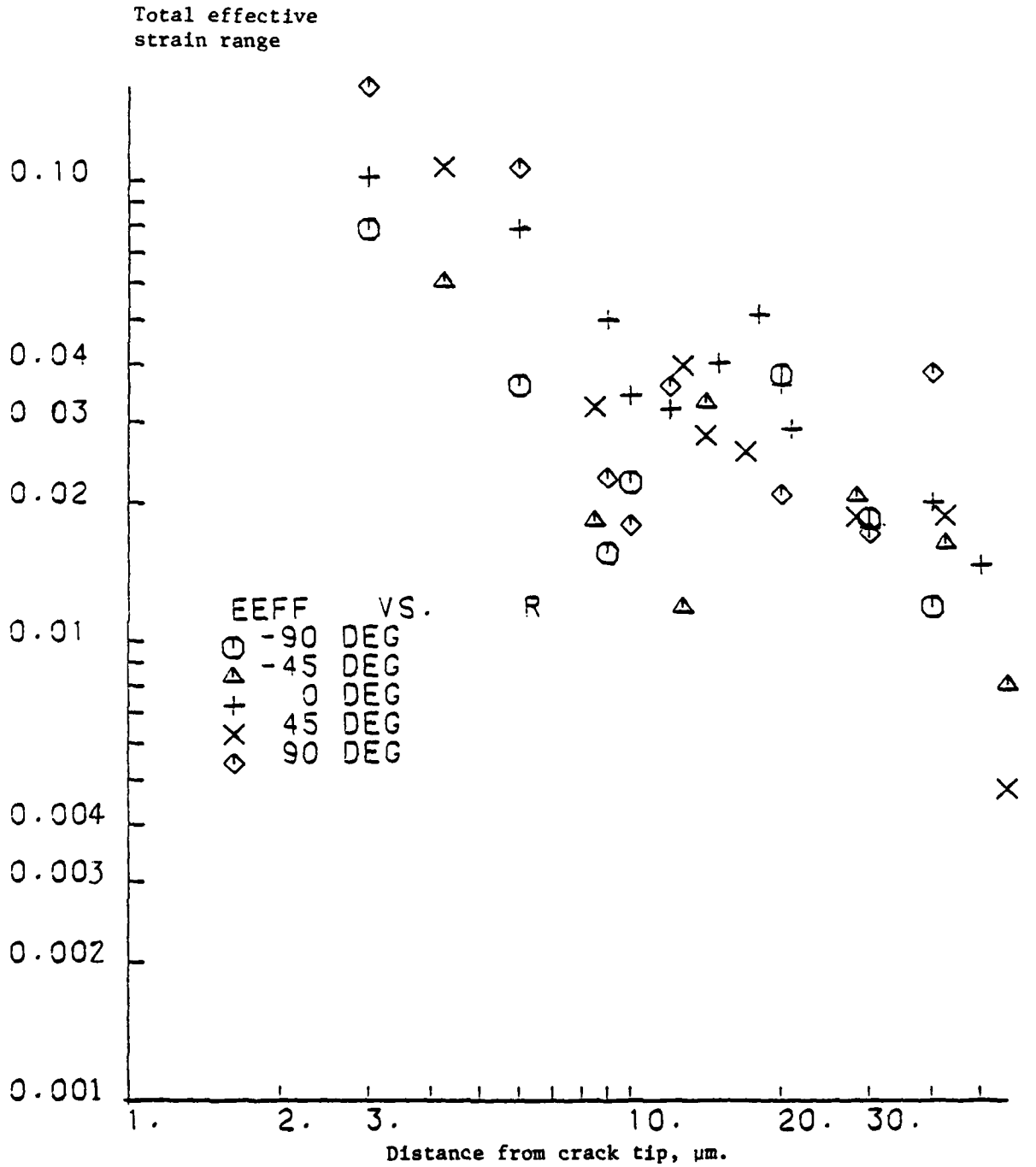

Figure C4. Total effective strain range vs distance from crack tip, Set 45.

UNCLASSIFIED

SECURITY CLASSIFICATION OF THIS PAGE (When Data Entered)

REPORT DOCUMENTATION PAGE	READ INSTRUCTIONS BEFORE COMPLETING FORM
1. REPORT NUMBER	2. GOVT ACCESSION NO. AD-A105 529 / 3. RECIPIENT'S CATALOG NUMBER
4. TITLE (and Subtitle) CRACK TIP PLASTICITY ASSOCIATED WITH CORROSION ASSISTED FATIGUE	5. TYPE OF REPORT & PERIOD COVERED Interim Report June 1980 - June 1981
	6. PERFORMING ORG. REPORT NUMBER 02-4268
7. AUTHOR(s) D. L. Davidson J. Lankford	8. CONTRACT OR GRANT NUMBER(s) N00014-75-C-1038
9. PERFORMING ORGANIZATION NAME AND ADDRESS Southwest Research Institute P. O. Drawer 28510 San Antonio, TX 78284	10. PROGRAM ELEMENT, PROJECT, TASK AREA & WORK UNIT NUMBERS 02-4268 NR 036-109/2-25/76(471)
11. CONTROLLING OFFICE NAME AND ADDRESS Office of Naval Research 800 North Quincy Street Arlington, VA 22217	12. REPORT DATE September 18, 1981
	13. NUMBER OF PAGES 44 + Prelims.
14. MONITORING AGENCY NAME & ADDRESS(if different from Controlling Office)	15. SECURITY CLASS. (of this report) UNCLASSIFIED
	15a. DECLASSIFICATION/DOWNGRADING SCHEDULE

16. DISTRIBUTION STATEMENT (of this Report)

Reproduction in whole or in part is permitted for any purpose of the United States Government. Distribution is unlimited.

17. DISTRIBUTION STATEMENT (of the abstract entered in Block 20, if different from Report)

18. SUPPLEMENTARY NOTES

19. KEY WORDS (Continue on reverse side if necessary and identify by block number)

Corrosion fatigue
Crack tip plasticity
Fatigue-environment interaction
Fatigue crack propagation
Crack tip strains
Aluminum alloys

20. ABSTRACT (Continue on reverse side if necessary and identify by block number)

Preliminary data is presented on the affect of a water vapor environment on the deformation within the plastic zone of fatigue cracks in 7075-T6. Results in the water vapor environment is compared to those in a vacuum environment. High spatial resolution observations have been made using a special cyclic stage for the SEM and strains have been determined using the stereoimaging technique. Crack tip opening is shown to be a power function of the distance behind the crack tip, in agreement with a theoretical derivation of this correlation. The crack tip strain correlates with the crack

DD FORM 1 JAN 73 1473 EDITION OF 1 NOV 65 IS OBSOLETE

UNCLASSIFIED

SECURITY CLASSIFICATION OF THIS PAGE (When Data Entered)

opening at 1 micrometer behind the crack tip. Crack tip strains are shown to vary considerably for a fixed cyclic stress intensity. By ignoring some data, a preliminary analysis is made which indicates that the water vapor environment lowers crack tip strains. Strain distribution within the plastic zone is shown to fit a logarithmic function, as opposed to a power function, although there is still some uncertainty in this result. Work on 7075-T6 and the powder metallurgy alloy MA-87 is continuing, with definitive results expected next year.

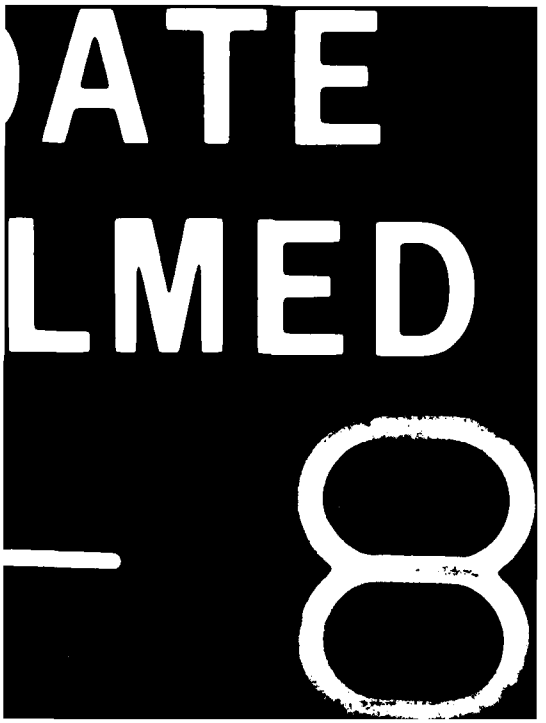
ATE
LMED
8